UNIVERSIDADE FEDERAL DO RIO GRANDE DO NORTE
CENTRO DE CIÊNCIAS EXATAS E DA TERRA
DEPARTAMENTO DE FÍSICA
GRADUATE PROGRAM IN PHYSICS

3+1 formalism in General Relativity

Tibério Azevedo Pereira

Natal-RN
April, 2018

Tibério Azevedo Pereira

3+1 formalism in General Relativity

Dissertation submitted in partial fulfilment of the requirements for the degree of master of Physics in the Departamento de Física of the Universidade Federal do Rio Grande do Norte.

Advisor
Prof. Dr. Raimundo Silva Junior

Universidade Federal do Rio Grande do Norte - UFRN

Departamento de Física - DF

Natal-RN
April, 2018

Universidade Federal do Rio Grande do Norte - UFRN
Sistema de Bibliotecas - SISBI
Catalogação de Publicação na Fonte. UFRN - Biblioteca Central Zila Mamede

Pereira, Tibério Azevedo.
3+1 formalism in General Relativity / Tibério Azevedo Pereira. - 2018.
87 f.: il.

Dissertação (mestrado) - Universidade Federal do Rio Grande do Norte, Centro de Ciências Exatas e da Terra, Pós-Graduação em Física. Natal, RN, 2018.
Orientador: Prof. Dr. Raimundo Silva Junior.

1. Gravitação - Dissertação. 2. Relatividade geral - Dissertação. 3. Formalismo 3+1 - Dissertação. 4. Relatividade numérica - Dissertação. I. Junior, Raimundo Silva. II. Título.

RN/UF/BCZM CDU 530.12

Elaborado por Ana Cristina Cavalcanti Tinôco - CRB-15/262

This dissertation is dedicated to my parents and my brother.

Acknowledgements

My thanks to UFRN for a pleasant academic environment. The whole staff of the Department of Physics, and especially the professors who contributed to my training. I thank my advisor for supporting my decision to do this dissertation whose subject is unusual to our field of study. I am thankful to the Clube do Fanfarrão and other friends for the good time in our everyday routines. I am grateful to CNPq for the financial support.

"Oh leave the Wise our measures to collate
One thing at least is certain, LIGHT has WEIGHT
One thing is certain and the rest debate
Light-rays, when near the Sun, DO NOT GO STRAIGHT."
(Arthur Eddington)

Abstract

The study of new solutions in General Relativity motivated investigations of Cauchy problems for alternative gravitational regimes, which led to the need to elaborate techniques to split the spacetime into three plus one dimensions. The 3+1 formalism arises as a mathematical tool for decomposing the components of the metric and the curvature. The central mechanism found in the literature is known as the ADM formalism, developed initially as an attempt to construct a theory of canonical quantum gravity, which later its formulation was applied to evolve the Einstein equation numerically. As a subfield of Gravitation, the Numerical Relativity investigates phenomena in strong field systems and other scenarios which are not possible to solve analytically. In this dissertation, we will present an introduction to the 3+1 formalism, as well as gauge and initial conditions to prepare some gravitational systems. To consolidate this theoretical approach, we will show techniques of Numerical Relativity to evolve the spacetime from of given initial configurations.

Keywords: Gravitation, General Relativity, 3+1 formalism, Numerical Relativity.

Resumo

O estudo de novas soluções na Relatividade Geral motivou investigações de problemas de Cauchy para regimes gravitacionais alternativos, o que levou à necessidade de elaborar técnicas para dividir o espaço-tempo em três mais uma dimensões. O formalismo 3+1 surge como ferramenta matemática para decompor as componentes da métrica e da curvatura. O mecanismo central encontrado na literatura é conhecido como o formalismo ADM, desenvolvido inicialmente como tentativa de construir uma teoria da gravidade quântica canônica, que mais tarde sua formulação foi aplicada para evoluir numericamente a equação de Einstein. Como um subcampo da Gravitação, a Relatividade Numérica investiga fenômenos em sistemas de campo fortes e outros cenários que não são possíveis de serem resolvidos analiticamente. Nesta dissertação, apresentaremos uma introdução ao formalismo 3+1, bem como condições iniciais e de calibre para preparar alguns sistemas gravitacionais. Para consolidar essa abordagem teórica, mostraremos técnicas de Relatividade Numérica para evoluir o espaço-tempo a partir de determinadas configurações iniciais.

Palavras-chave: Gravitação, Relatividade Geral, Formalismo 3+1, Relatividade Numérica.

Contents

Chapter 1

Introduction

Gravity. From ancient thinkers in 400 BC, the phenomenon of free fall had already put them in question about the nature of matter and its behaviour in the World. Greek philosophers discussed classifications for the matter to explain their motion concerning to the centre of the Universe (Earth) [1, 2]. Later in 500 BC, Indian geometricians and astronomers include the movement of celestial bodies as gravitational phenomena and the initial concepts of "attractive force" were debated [3, 4].

In the Modern era, the English natural philosopher Isaac Newton, inspired by his contemporaneous, formulate the "Law of Universal Gravitation" [5]. Such imposing name for a long time was said as the best theory of gravity. It describes the elliptical orbits of planets, tidal forces; from his equation, we predicted the existence of the planet Neptune [6], and it made possible the space race which took the human being to the Moon [7]. Until the 1900s, Newton's gravity faced only an imprecise measure, the Mercury's perihelion precession.

In 1905, Physics expanded its fields to include new effects of mechanics on bodies at high speed. After Einstein's Special Theory of Relativity, the classical equations were reformulated to incorporate relativistic corrections and also the concept of mass-energy equivalence. However, at that time, physicists had not yet found any gravitational system in relativistic regime [8].

The study of the reference frame in freely-falling bodies and analyses of gravitational and inertial mass relationship allowed Albert Einstein to note a gap in classical gravity.

His efforts to understand further Gravity took him to a geometrical description of the spacetime, in which dynamical equations evolve the components of the metric tensor. The theory of General Relativity (GR) is nowadays the best theory that predicts more phenomena in astrophysical and cosmological scale.

The study of Cauchy problems in GR to investigate solutions for different gravitational systems has always motivated research in Gravitation [9, 10]. In 1962, R. Arnowitt, S. Deser and C. W. Misner stimulated by these works purposed a quantum description of Einstein equation written in spacelike canonical tensors [11]. Their theory of quantum gravity requires splitting spacetime into space and time, as a 3+1 formalism technique. The specific definitions ascribed by the authors become known as the ADM formalism.

Later, the ADM formalism became an essential tool for numerical solutions of Einstein equation. Usually, in numerical simulations, differential equations are solved in each point of a three-dimensional grid for each timestep. The set of grids along the time interval compose the fourth dimension of the system, the time flow. The similarity with the decomposition established by the ADM formalism allows us to obtain numerical solutions of strong gravitational regimes which would not be possible with non-relativistic gravity, such as black hole mechanics. The sample of techniques to simulate 3+1 GR is so-called Numerical Relativity (NR), as a subfield of Gravitation [12].

In this dissertation, we will review some aspects of General Relativity in Chapter 2 to apply this knowledge in 3+1 formalism. In Chapter 3, we will introduce this formalism and obtain the ADM set of equations. To understand their straight application, in Chapter 4 we will treat gauges and initial conditions for different regimes. Finally, in Chapter 5, we will produce numerical experiments as an application of Numerical Relativity. Throughout this dissertation, we will assume the metric signature "-2" $(+\,,-\,,-\,,-\,,-\,)$. Also, Greek indexes imply spacetime tensor elements ($\mu = 0, 1, 2, 3$) and Latin ones, three-dimensional spatial quantities ($i = 1, 2, 3$).

Chapter 2

A brief review on General Relativity

At the beginning of our discussion, we will relive the occasion that led a very talented and creative physicist to have one of his first insights into the nature of Gravity. We go back to 1907 in the city of Bern, the capital of Switzerland, in which one day Albert Einstein was working in a patent office when a fatal accident with a roofer happened. This tragic event motivated Einstein to think about the relationship between body and gravitational acceleration, what he called *"the happiest thought of my life"*. After that, he began a furious investigation about the relativistic behaviour of Gravity, which took him eight years to give rise to the *General Theory of Relativity* [13].

2.1 The Equivalence Principle

The fall of the roofer was probably one of his first thought experiments related to gravitation. The set of these "experiments", in an attempt to apply the knowledge of Special Relativity to the gravitational phenomena, is known as the Einstein Equivalence Principle (EEP). It is common to find in literature a division of the principle into two categories, the "weak" (WEP) and "strong" (SEP) versions. Here, we will not explore the EEP using this division, we will discuss it with some thought experiments in which both characteristics will be analysed.

Our thought experiments start by imagining a physicist in free fall. In his frame of reference, the feeling of weight does not exist, and the experience could be compared

intuitively to an astronaut drifting in the cosmic space. As illustrated in Fig. 2.1, a free-falling body under the gravitational acceleration $\vec{g}$ presents the equivalent effect of a body free of a gravitational field. This means that $\vec{g}$ may not exist if we had a changing of scenario, *i.e.*, it is possible to write the total force of the case A as $\vec{F}_A = -m\vec{\nabla}\phi$ and for the case B, $\vec{F}_B = \vec{0}$.

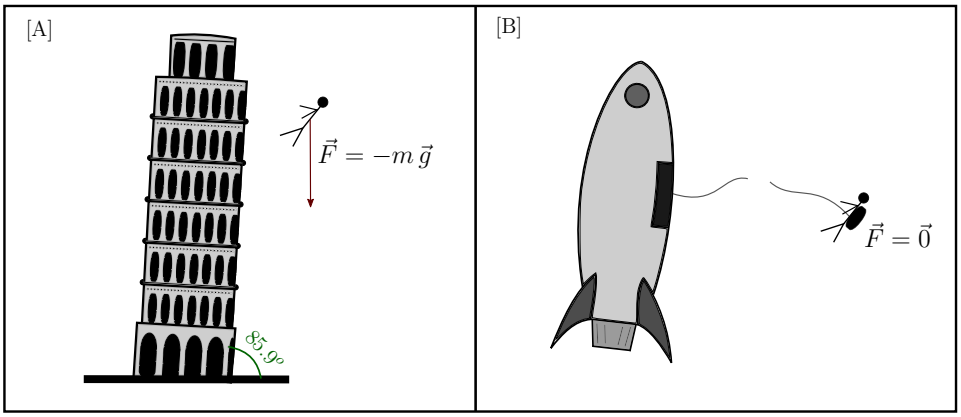

Figure 2.1: The figure A shows a free-falling body under a gravitational field $\vec{g}$. The figure B represents an astronaut in such reference frame free of (significant) gravitational interaction.

We will investigate whether the body's mass has a mechanism analogous to an induced charge, as it happens in electrical interactions. The parallel between electrical and gravitational forces (one-dimensional) can be described as

$$F_g = m_i\,\ddot{x} = -m_g\,\partial_x\phi_g\,, \tag{2.1}$$

$$F_e = m_i\,\ddot{x} = -q\,\partial_x\phi_e\,. \tag{2.2}$$

Here, m_i is the inertial mass and m_g is the gravitational charge/mass. The force F_e describes a particle with mass m_i and electric charge q under the action of the potential ϕ_e. We already know that an electrically neutral material – a conductor – can give rise to an electric potential when an external charge q is present. Otherwise, for the force F_g, a particle of mass m_i and gravitational charge m_g is under the potential ϕ_g. However, do massive particles present gravitational charges that can be induced by a second body? Is m_g another intrinsic property of matter as well as m_i and q?

Different from the charge-to-mass ratio, $q/m_e \simeq -1.758 \times 10^{11}\, C/kg$ (for an electron), experiments show inertial mass and gravitational charge are equal quantities, $m_g/m_i = 1$[1]. Therefore, seeing that there is no gravitational charge responsible for the bodies attraction, $\vec{x} = \vec{g}$ can be seen as just an accelerated reference frame. And then, we may doubt that gravitation perhaps would not be a phenomenon of an inherent property of the body, but the reflection of something out of it, which also takes account to the relativistic effect of the body's acceleration. This aspect we will discuss later with the advanced Einstein's ideas about his gravitational theory.

For complementary analysis, in another thought experiment, an astronaut is under the acceleration of a starship far from any other body. This case is equivalent to the situation of a physicist under Earth's (quasi-uniform) gravitational force [14].

In short, the Equivalence Principle tells us, for a broader point of view, that any experiment cannot distinguish a gravitational field from an accelerated frame of reference. However, this sentence is only correct when the system requires measurements in a short interval of space and time, since tidal forces could be detected, and then gravity could be spotted. Roughly speaking, locally, acceleration is equal to Gravity.

Two remarkable phenomena of Einstein's theory of gravity can be taken from the EEP. We can imagine an elevator at high upward acceleration with a laser beam coupled in one of its walls, frequently emitting pulses of light parallelly to the floor, see Fig. 2.2. From an inertial reference frame out of the elevator, an observer sees the first pulses coming down while the elevator moves fast upward. As a consequence of the EEP, the elevator's acceleration is equivalent to a gravitational effect on the situation which the light bends around a massive body.

To verify the second phenomenon, we will still work on our imaginary elevator. Now, the elevator has a laser beam on the floor pointing up, and another on the ceiling pointing downward, and each laser has an observer with a clock on its opposite side. Both clocks are synchronised at the beginning of the acceleration, pictured in Fig. 2.3. When the

[1]The best-known experiment is called *Eötvös experiment*, developed by the Hungarian physics Loràand Eötvös. The high accuracy is its main feature used to measure the ratio between inertial and gravitational mass in an elaborated torsion balance.

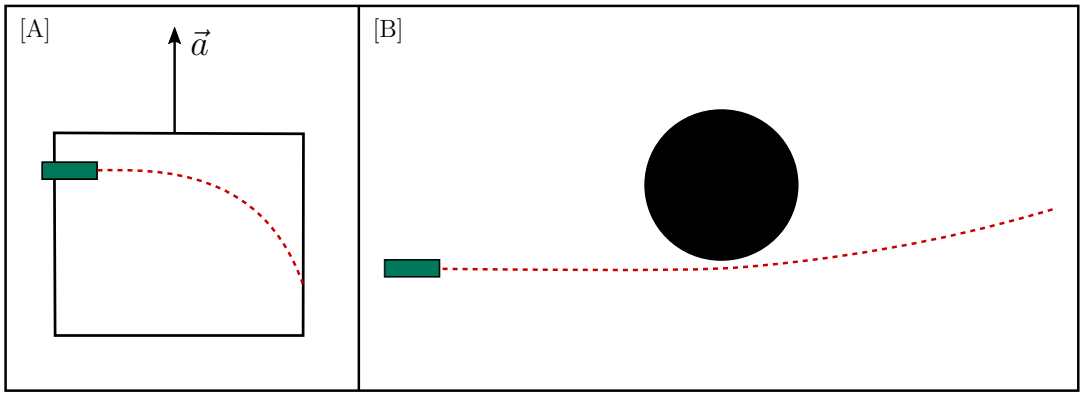

Figure 2.2: In A, one shows an elevator at high upward acceleration such as an observer out of it could notice the light pulses coming down. Likewise, B represents a light ray deflected by a massive body.

elevator moves, an observer from the top receives the pulse slower than the observer from the bottom. However, considering the second postulate of Special Relativity – the constancy of the speed of light – what is happening is that the time dilation effect is more significant to the clock at the bottom than to the top one. The EEP guarantees that a clock close to a massive body runs slower than a clock far from it. The twin paradox also could be applied to twins on different planets with a discrepant mass difference.

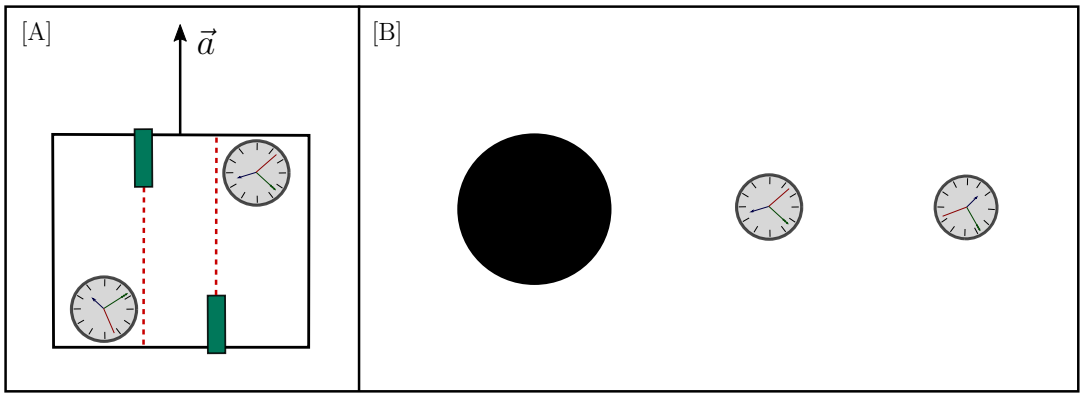

Figure 2.3: The illustration A presents the simultaneous time measurements of the light pulse going to observers with clocks. As the elevator moves with acceleration $\vec{a}$, both observers will measure different effects of time dilation. It also can be seen in figure B, in which clocks run slower close to a massive body.

2.2 Gravitational dynamics

During the year of 1911, in Prague, Einstein gave progress to his insights about gravity. In his thoughts, the changing of a reference frame, at that moment, could invalidate the gravitational acceleration as it also happens with fictitious forces. The position of an object and its observer on space(time) was something actively investigated by him, and the Dutch physicist Hendrik Lorentz, in the Special Theory of Relativity. Moreover, the German mathematician Hermann Minkowski, who had been Einstein's teacher, had already established the concept of *spacetime* and its geometry.

Einstein started to look for a new dynamical equation similar to the Poisson equation (2.3), but it somehow would be generalised to the relativistic regime and take into account the geometry of spacetime, in other words, it would have to be Lorentz invariant. The left-hand side of Eq. (2.3), should have a second time derivative, characteristic which is present in dynamical equations. Meanwhile, his intuition pointed to differential geometry – the Gauss theory of surfaces – in particular, the analysis of the physical meaning of the coordinates in these surfaces.

$$\nabla^2\phi = 4\pi G\,\rho\,. \tag{2.3}$$

Later, when Einstein returned to work in Zurique, he asked a friend to help him clarify his studies on manifold geometry, he was seeking a way to describe gravity geometrically. His friend was the Hungarian mathematician Marcel Grossmann who introduced to Einstein the works of three brilliant mathematicians, Bernhard Riemann, Ricci-Curbastro and Levi-Civita. The collaboration with Grossmann was essential to build the first formulations of the theory; however, there was someone else who also guided Einstein's research, his first wife, Mileva Marić[2].

After Max Planck's invitation to become a member of the Prussian Academy of Sciences in Berlin, in 1914, Einstein already had an early version of his gravitational

[2]Mileva Marić was a Serbian physicist. Her exceptional ability in mathematics was crucial to solving most of the mathematical problems in the early steps to the elaboration of the General Theory of Relativity [15].

theory as a tensorial equation. It was previously known that the components of energy (mass, momentum and energy flux) could be compressed into the energy-momentum tensor $T_{\mu\nu}$ and the conservation's law of energy-momentum obeys $\nabla_\mu T^{\mu\nu} = 0$. Therefore, the right-hand side of Einstein equation should be proportional to $T_{\mu\nu}$. The left-hand side (the geometrical part), however, it was intensively worked out to correspond to Poisson equation in the weak field limit and to compute the correction of the precession of Mercury's perihelion.

The studies of Riemann curvature tensor led Einstein to a remarkable consequence of the *Bianchi identity*, the contracted form given by $\nabla_\mu \left(R^{\mu\nu} - \frac{1}{2} R\, g^{\mu\nu}\right) = 0$. Thereby, the right and left-hand parts are joined by a constant. On 25 November 1915, Einstein published the complete version of the dynamic equation of gravitation [16],

$$R_{\mu\nu} - \tfrac{1}{2} R\, g_{\mu\nu} = \kappa\, T_{\mu\nu}\,. \tag{2.4}$$

Meanwhile, five days before, the German mathematician David Hilbert presented a form for Einstein equation by using the *Variational Principle*. What Hilbert found was the Lagrangian of the geometrical part of the field equation, *i.e.*, the sourceless condition, $T_{\mu\nu} = 0$. The complete form is described by the action,

$$S = \int \left(\frac{1}{2\kappa} R + L_m\right) \sqrt{-g}\, d^4x\,. \tag{2.5}$$

The first experimental test result, the perihelion precession of Mercury, was published in the paper of 1915. The phenomenon of light deflection was confirmed in 1919, and many others were measured with satisfactory accuracy as the gravitational redshift, accretion disk around compact objects and frame-dragging. Nonetheless, there was still a phenomenon that Einstein equation did not predict, thanks to the astronomers Vesto Slipher and Edwin Hubble, in 1929 the final measurements of the *expansion* of the Universe could be taken [17, 18]. Thus, Einstein had to do one more modification in his

equation. The final version of the field equation of gravity is

$$G_{\mu\nu} + \Lambda\, g_{\mu\nu} = \kappa\, T_{\mu\nu}\,. \tag{2.6}$$

The last observation, that confirmed a remarkable phenomenon predicted by Einstein, was the detection of gravitational waves. The linearised approach of the field equation leads to a wave equation which govern the propagation of small spacetime ripples – detected by interferometers in 2015 [19].

2.2.1 The meaning of Einstein field equation

Understanding the meaning of Einstein equation is not an easy task [20]. Here, we will highlight our comprehension for each tensorial component of the field equation. Firstly, we will investigate the physical units that compose Eq. (2.6).

The geometrical part expresses the Einstein tensor, $G_{\mu\nu} \doteqdot R_{\mu\nu} - \frac{1}{2}R\, g_{\mu\nu}$, and the *cosmological constant* Λ. The Ricci tensor,

$$R_{\mu\nu} = \partial_\sigma \Gamma^\sigma_{\mu\nu} - \partial_\nu \Gamma^\sigma_{\mu\sigma} + \Gamma^\rho_{\mu\nu}\,\Gamma^\sigma_{\rho\sigma} - \Gamma^\rho_{\mu\sigma}\,\Gamma^\sigma_{\rho\nu}\,, \tag{2.7}$$

is defined regarding the connection coefficients (Christoffel symbol),

$$\Gamma^\sigma_{\mu\nu} = \tfrac{1}{2} g^{\sigma\rho}(\partial_\nu g_{\rho\mu} + \partial_\mu g_{\nu\rho} - \partial_\rho g_{\mu\nu})\,, \tag{2.8}$$

which takes into account a torsionless spacetime. Since the metric $g_{\mu\nu}$ has no unit, its partial derivative presents the inverse length dimension, so $[\Gamma^\sigma_{\mu\nu}] = m^{-1}$. Consequently, $[R_{\mu\nu}] = m^{-2}$ as well as the whole geometrical part of Einstein equation. The unit of the constant κ depends on how we define the energy-momentum tensor's unit; thus we will establish its unit for energy density, $[T_{\mu\nu}] = m^{-3}\, J$. Thereby, the coupling constant is defined as $\kappa \doteqdot 8\pi\, G/c^4$ and $[\kappa] = kg^{-1}m^{-1}s^2 = m\, J^{-1}$.

The dynamics described by Eq. (2.6) can be clearly noted when we express the Ricci tensor (2.7) using the relation (2.8) to give rise to the second derivatives of the metric.

Einstein equation is then said *field equation* because each component of $g_{\mu\nu}$ acts as a scalar field. The metric tensor, introduced by Riemann, is intrinsically related to the distance between two events on spacetime. The line element, $ds^2 = g_{\mu\nu}\, dx^\mu dx^\nu$ reveals that $g_{\mu\nu}$ is responsible for the length measurement in a chosen coordinate system.

To evaluate Einstein tensor, let us analyse the Riemann (curvature) tensor. By definition, it can be assimilated as the measure of how much a given vector v changes its direction when it is parallel transported on the boundaries of an infinitesimal loop [21], that is written as $R^\rho{}_{\sigma\mu\nu}\, v^\sigma = [\nabla_\mu, \nabla_\nu]\, v^\rho$. On the other hand, its contracted form – the Ricci tensor – takes into account the displacement of an infinitesimal volume along a geodesic [22]. The unit of volume is seen evidently when, in Eq. (2.6), the Ricci tensor is expressed proportionally to the energy density as in the following form,

$$R_{\mu\nu} = \kappa \left(T_{\mu\nu} - \tfrac{1}{2} T\, g_{\mu\nu} \right) + \Lambda g_{\mu\nu} \,. \tag{2.9}$$

The Ricci scalar – or scalar curvature – determines how much the area of a 3-sphere, for instance, embedded in a curved spacetime is distorted concerning to a flat spacetime. Composing the Einstein tensor, in Eq. (2.6), we may deduce that curvature holds energy. The cosmological term $\Lambda\, g_{\mu\nu}$ includes, in the dynamics of the system, the expansion of the Universe as a repulsive or attractive gravitational effect. For a global interpretation of Einstein equation, the American physicist John Wheeler said:

Matter tells spacetime how to curve; spacetime tells matter how to move.

The right-hand side of the Eq. (2.6) takes into account the energetical contribution of the environment. The energy-momentum tensor is the input of the considered system, and then, the metric fields are the output, *i.e.*, how spacetime behaves. For a given matter (energy) action S_m, the energy-momentum tensor is generalised to

$$T_{\mu\nu} \doteqdot \frac{-2}{\sqrt{-g}} \frac{\delta S_m}{\delta g^{\mu\nu}} \,. \tag{2.10}$$

If we consider that our system contains only a perfect fluid – with density ρ, pressure p and four-velocity u^σ – the energy-momentum tensor takes the form of Eq. (2.11).

However, in the case of the presence of electromagnetic fields, $T_{\mu\nu}$ is written in terms of the *electromagnetic tensor* $F^{\mu\nu}$, Eq. (2.12). Further, we could be interested in working with a scalar field ϕ, related to a potential $V(\phi)$, as seen in Eq. (2.13).

$$T_{\mu\nu}^{(fluid)} = \left(\rho + p\,c^{-2}\right) u_\mu u_\nu + p\, g_{\mu\nu}\,, \tag{2.11}$$

$$T_{\mu\nu}^{(EM)} = \mu_0^{-1}\left(F_{\mu\sigma}F_{\nu}{}^{\sigma} - \tfrac{1}{4}\, g_{\mu\nu}\, F_{\rho\sigma}F^{\rho\sigma}\right)\,, \tag{2.12}$$

$$T_{\mu\nu}^{(\phi)} = \partial_\mu\phi\,\partial_\nu\phi - g_{\mu\nu}\left[\tfrac{1}{2}\,\partial_\sigma\phi\,\partial^\sigma\phi + V(\phi)\right]\,. \tag{2.13}$$

Another point for discussing is a remarkable consequence of Einstein equation structure, its *nonlinearity*. According to the Equivalence Principle, inertial and gravitational masses are the same property of matter; thus – for the total gravitational energy of a binary particle system – besides including the energy of the mutual attraction of the particles, one also has to consider the resting energy of each one. Since the *superposition principle* is not enough to compute relativistic corrections, the field equation is said nonlinear. Physically, it means that not only mass-energy gravitate but also *gravity couples with itself*.

2.2.2 Some exact solutions

The exact solutions of Einstein equation are taken for some specific regimes and symmetries. The first solution was found by the German physicist Karl Schwarzschild, in 1916, in a trench during the World War I. His *vacuum* solution improved the comprehension of the spacetime geometry, as verified by the observation of the light deflection and several other experiments.

The Schwarzschild solution takes into account the region out of the source, as well as the Laplace equation [23]. Thus, the solution for $R_{\mu\nu} = 0$ in a spherically symmetric spacetime[3] gives us the metric described by the line element,

$$ds^2 = -\left(1 - \frac{r_s}{r}\right)c^2dt^2 + \left(1 - \frac{r_s}{r}\right)^{-1}dr^2 + r^2d\Omega^2\,, \tag{2.14}$$

[3]According to the *Birkhoff theorem*, any spherically symmetric spacetime is described by Schwarzschild geometry and, as a consequence, the metric will be stationary [24].

where $r_s \doteqdot 2MG/c^2$ is the *Schwarzschild radius* (in terms of the mass M of the body, the gravitational constant G and the constant speed of light c) and $d\Omega^2 = d\theta^2 + \sin^2\theta\, d\phi^2$. The metric presents singularity at $r = 0$, where GR cannot give us any information about this point and its surroundings in quantum scale. However, a body collapsed in a radius shorter than r_s is characterised as a *black hole* and its geometry is constantly studied in different coordinate systems. In particular, the *isotropic* radial coordinates, $r \to r\,(1 + r_s/4r)^2$, carries a notable mathematical consequence, the spatial part of the metric,

$$ds^2 = -\left(\frac{1 - r_s/4r}{1 + r_s/4r}\right)^2 c^2 dt^2 + \left(1 + \frac{r_s}{4r}\right)^4 \eta_{ij}\, dx^i\, dx^j\,, \tag{2.15}$$

is expressed by a scalar field coupled with a flat space, inherent to a *conformal metric* [25].

In Schwarzschild geometry, we may represent its curvature in the *embedded diagram*. Considering only the radial and azimuthal coordinates of (2.14) and comparing with the spatial line element in cylindrical coordinates, $dl^2 = d\rho^2 + \rho^2 d\phi^2 + dz^2$, we find that $z(r) = 2\sqrt{r_s(r - r_s)}$. Therefore, the z-axis portrays the curvature of the spatial "slice" of the spacetime (see Fig. 2.4).

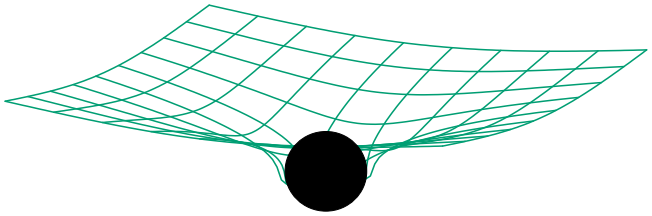

Figure 2.4: The embedded diagram represents the magnitude of the constriction of the spacetime – in the surrounding a massive body – in the z-axis of the cylindrical coordinate system.

If now we consider rotating bodies, the metric cannot hold spherical symmetry since the spacetime would have to be symmetric in the azimuthal coordinate and non-time symmetric ($t \to -t$). The *Kerr solution* brings these elements in the following metric,

$$ds^2 = -\frac{\rho^2\Delta}{\Sigma^2}c^2 dt^2 + \frac{\Sigma^2 \sin^2\theta}{\rho^2}(d\phi - \omega\, dt)^2 + \frac{\rho^2}{\Delta}dr^2 + \rho^2 d\theta^2\,, \tag{2.16}$$

which is written in *Boyer–Lindquist coordinates*,

$$\begin{aligned} \rho^2 &= r^2 + a^2 \cos^2\theta \,, \\ \Delta^2 &= r^2 - r_s r + a^2 \,, \\ \Sigma^2 &= (r^2 + a^2)^2 - a^2 \Delta \sin^2\theta \,, \end{aligned}$$

and the constant $\omega = a r_s r c/\Sigma^2$ and $a = J/Mc$ are related to the angular momentum J [26]. In the limit $a \to 0$, the quantities $\Delta \to r^2(1 - r_s/r)$, $\rho^2 \to r^2$ and $\Sigma^2 \to r^4$ recover Scharwzschild metric.

The metric in the form (2.16) is a modern reformulation in spherical coordinates. The "original" version published by Roy Kerr in 1963 is given by

$$ds^2 = (\eta_{\mu\nu} - \lambda\, l_\mu l_\nu) dx^\mu dx^\nu \,. \tag{2.17}$$

The so-called *Kerr-Schild form* relates the null vector l_μ, so $l_\mu l^\mu = 0$, and it is defined in cartesian coordinates as

$$l_\mu = \left(c, \frac{rx + ay}{a^2 + y^2}, \frac{ry - ax}{a^2 + y^2}, \frac{z}{r} \right) , \tag{2.18}$$

where $r^2 = x^2 + y^2 + z^2$. The function λ is also a function of the angular momentum J, such that $\lambda = r_s r^3/(r^2 + a^2 z^2)$.

Now, we again search for spherically symmetric solutions, but considering the isotropic density and pressure of a perfect fluid. The energy-momentum tensor takes the form of Eq. (2.11) and the metric is

$$ds^2 = -A(r)\, c^2 dt^2 + \left[1 - \frac{2Gm(r)}{c^2\, r} \right]^{-1} dr^2 + r^2 d\Omega^2 \,, \tag{2.19}$$

in which the mass $m(r)$ is a function of the density ρ,

$$m(r) = 4\pi \int_0^r \rho(\bar{r})\, \bar{r}^2 d\bar{r} \,. \tag{2.20}$$

The radial function $A(r)$ obeys

$$\frac{A'}{A} = -\frac{2p'}{\rho c^2 + p}\,, \tag{2.21}$$

where the prime stands for the total derivative. To obtain a solution for the radial function $A(r)$, we derive the *Oppenheimer–Volkoff equation* responsible to compute the radial derivative of the pressure $p'(r)$ [27],

$$\frac{dp}{dr} = -\frac{1}{r^2}(\rho c^2 + p)\left[\frac{4\pi G}{c^4}pr^3 + \frac{2Gm(r)}{c^2}\right]\left[1 - \frac{2Gm(r)}{c^2\, r}\right]^{-1}\,. \tag{2.22}$$

All these solutions are in the astrophysical regime since the cosmological constant can be negligible. However, in the Friedmann–Robertson–Walker (FRW) metric we consider an expanding spacetime wherein the whole material content of the Universe is interpreted as a perfect fluid [28],

$$ds^2 = -c^2dt^2 + a(t)^2\left(\frac{dr^2}{1-kr^2} + r^2 d\Omega^2\right)\,. \tag{2.23}$$

Here, $a(t)$ is the *scale factor* and k is the constant that signals the curvature of the universe. The solutions that govern the evolution of the cosmic fluid are

$$\left(\frac{\dot{a}}{a}\right)^2 = \frac{8\pi G}{3}\rho - \frac{c^2k}{a^2} + \frac{1}{3}\Lambda c^2\,, \tag{2.24}$$

$$\frac{\ddot{a}}{a} = -\frac{4\pi G}{3}\left(\rho + \frac{3p}{c^2}\right) + \frac{1}{3}\Lambda c^2\,. \tag{2.25}$$

The constant Λ can be seen as a component of energy – when the energy-momentum tensor incorporates it – known as *dark energy*.

2.3 Kinematics on spacetime

Up to here, we have discussed – according to Wheeler's quotation – how matter curves spacetime (what metric expresses a given environment), but now, we will talk about

how spacetime moves matter. The dynamics tell us how the metric (spacetime) evolves; the kinematics gives us the sources equations of motion.

These equations of motion are usually derived by the conservation of the energy-momentum tensor, $\nabla_\mu T^{\mu\nu} = 0$. The least length between two events in a (pseudo)-Riemannian manifold[4] is led by *geodesics*. So, we can deduce the geodesic equation for particles using the pressureless form of Eq. (2.11), $\nabla_\mu(\rho\, u^\mu\, u^\nu) = u^\mu \nabla_\mu u^\nu = 0$, and then we obtain,

$$\ddot{x}^\sigma + \Gamma^\sigma_{\mu\nu}\, \dot{x}^\mu\, \dot{x}^\nu = 0\,. \tag{2.26}$$

On the other hand, if we consider a fluid with inner pressure we will derivate relativistic the *equation of motion* and the *equation of continuity*,

$$\left(\rho + p/c^2\right) u^\mu \nabla_\mu u^\nu + \left(g^{\mu\nu} + u^\mu u^\nu/c^2\right) \nabla_\mu\, p \;=\; 0\,, \tag{2.27}$$

$$\nabla_\mu\, (\rho u^\mu) + \frac{p}{c^2} \nabla_\mu u^\mu \;=\; 0\,. \tag{2.28}$$

The geodesic equation such as Eq. (2.26) describes *freely-falling* particles, *i.e.*, we are considering only the gravitational effect of the curved spacetime. For particles that are under the action of a given potential $V(x)$, we may evaluate the Lagrangian, $L = \frac{1}{2} g_{\mu\nu} \dot{x}^\mu \dot{x}^\nu - V(x)$, in the *Euler-Lagrange equation*,

$$\frac{\partial L}{\partial x^\mu} = \frac{d}{d\tau} \left(\frac{\partial L}{\partial \dot{x}^\mu} \right)\,, \tag{2.29}$$

to get the geodesic equation in the form,

$$\ddot{x}^\sigma + \Gamma^\sigma_{\mu\nu}\, \dot{x}^\mu\, \dot{x}^\nu = -g^{\sigma\rho} \partial_\rho V\,. \tag{2.30}$$

If the system contains charged particles, the electromagnetic fields are included in the electromagnetic tensor, as $\partial^\sigma V = -\dfrac{q}{m_0} F^\sigma{}_\rho\, \dot{x}^\rho$. For a scalar field ϕ, the equation of

[4] A Riemannian manifold is characterised by basis vectors $\vec{e}_a(x)$ which define the metric $g_{ab}(x) = \vec{e}_a \cdot \vec{e}_b$, and the line element such that $ds^2 = g_{ab}\, dx^a dx^b > 0$. Since in Special Relativity we may work with a timelike, spacelike or lightlike interval, in GR it is said that our manifold is *pseudo*-Riemannian.

motion is straightforwardly obtained applying the Lagrangian in the Euler-Lagrange equation to get the equation of motion, $\Box\phi = V'$ [5].

At this point of our discussion, we now can investigate how the geodesic equation works. To guide our analysis, let us suppose a freely-falling particle in a Schwarzschild spacetime that is at rest related to a source. What causes the particle acceleration? To answer this question, we will split Eq. (2.26) out into two parts,

$$\ddot{t} + \Gamma^0_{\mu\nu}\,\dot{x}^\mu \dot{x}^\nu = 0\,, \tag{2.31}$$

$$\ddot{x}^i + \Gamma^i_{\mu\nu}\,\dot{x}^\mu \dot{x}^\nu = 0\,. \tag{2.32}$$

Both equations, $\dot{x}^\mu \doteqdot dx^\mu/d\tau$, where τ is the *proper time*, the time at the particle's reference frame – the time along the geodesic. In the first equation, $t = x^0/c$ is the time measured by an observer out of the particle's geodesic. Therefore, this equation says how the observer's time t changes regarding to the geodesic's time τ. The second equation, otherwise, updates the particle's position in all three spatial directions – it accelerates the particle.

Once our particle is initially at rest, to simplify, we will examine only the radial direction ($x^1 = r$), and then $\dot{r} = 0$. Our equations reduce to,

$$g_{00}\,\dot{t}^{\,2} = k\,, \tag{2.33}$$

$$\ddot{r} + \Gamma^1_{00}\,\dot{t}^{\,2} = 0\,, \tag{2.34}$$

where the constant $k = E/(m_0c^2) = 1$. These equations are related to the moment immediately before the particle starts to accelerate. Defining $u \doteqdot \dot{r}$ and expanding the radial velocity as $u_{\tau+\Delta\tau} \simeq u_\tau + \Delta\tau\,\dot{u}_\tau$, we obtain that (for $u_\tau = 0$),

$$u_{\tau+\Delta\tau} \simeq -\Delta\tau\,\Gamma^1_{00}\,\dot{t}^{\,2}\,. \tag{2.35}$$

Through the relation above, we can deduce that there are two components responsible

[5] The d'Alembertian operator in curved spacetime is defined as $\Box \doteqdot \nabla_\mu\nabla^\mu$.

for the particle's acceleration, Γ^1_{00} and $\dot{t}$. The connection coefficients are defined regarding the basis vectors, $\Gamma^{\sigma}_{\mu\nu} = \vec{e}^{\,\sigma} \cdot \partial_\nu \vec{e}_\mu$, that can be thought as a collection of values of how the basis vectors, in a given point at the manifold, diverge from the orthogonality, which denotes the curvature. The term $\dot{t}$ is the rate in which the observer's clock runs related to the particle's clock. The thought is similar to the twin-paradox – how the time flows for each sibling – that tell us about the time dilation effect. Thereby, $\dot{t}$ measures the rate of time dilation between particle and observer. At this point, we may conclude that:

> *The gravitational acceleration of a particle at rest is due to the local curvature manifested by the rate of change of the basis vectors related to their coordinates, which therefore affects the rate of time dilation for the observed particle.*

Chapter 3

The 3+1 formalism

The elaboration of a four-dimensional geometry composed by three-dimensional space *plus* time is a remarkable achievement for Mathematics and Physics. The relativistic mechanics was initially the main target to implement the spacetime as a way to portray the change of reference frames. The French physicist Henri Poincaré was the first to include the (imaginary) temporal coordinate to the Euclidean space and treat the electron relativistic phenomena [29]. Later, Hermann Minkowski improved the description of the spacetime to manage four-dimensional vectors on manifolds, and so, time was defined as a real coordinate [30].

In Classical Field Theory, the Lagrangian formulation is invariant under Lorentz transformation, and spacetime plays an important role in this mechanism. However, in Hamiltonian formulation, the kinematic variables q_i and p_i are purely spacial, and they evolve for each time interval [31]. As a result, the canonical description needs to split spacetime in *3+1 form*. In General Relativity, the 3+1 techniques were pertinent to study *Cauchy problems* and, at some point, a manner of how to build the Hamiltonian of the Einstein equation as an attempt to express a quantum version of GR. This last investigation was published by R. Arnowitt, S. Deser and C. W. Misner in 1962 [11]. Their mathematical formulation has become known as the *ADM formalism*, that we will study in this chapter.

With the advance of Computer Science and the need to find numerical solutions of GR in strong field regime, the 3+1 formalism proves to be a bright proposal to split the

tensorial fields into a set of equations [32]. In deterministic simulations, in general, we need to evolve all these fields in each point of the *grid* to perform the next *timestep*. The logistics behind 3+1 formalism is the same; we slice up the spacetime into hypersurfaces for each instant of time to evaluate the field equations for each slice. The key of ADM formalism is how to carry these fields throughout the hypersurfaces.

3.1 Slices of spacetime

In GR, an observer experiment the laws of Physics in a four-dimensional manifold $\mathcal{M}$ described by the fields of the metric $g_{\mu\nu}$. The technique used in the ADM formalism, so-called *foliation*, consist of slicing up the spacetime $(\mathcal{M}, g_{\mu\nu})$ into three-dimensional spacelike hypersurfaces Σ_t of constant time, relative to the global *time function* $\mathfrak{t}$. As illustrated in Fig. 3.1, an *coordinate* observer at Σ_t remains his spatial coordinates constant through the vector $\vec{t}$ after a time "lapse" at Σ_{t+dt}. From the point of a *Eulerian* observer, that fallows the *normal vector* $\vec{n}$ (orthogonal to Σ_t), the coordinate observer is "shifted" to a distance $|\vec{\beta}|^2$ after a proper time interval $d\tau = \alpha\, cdt$ [33].

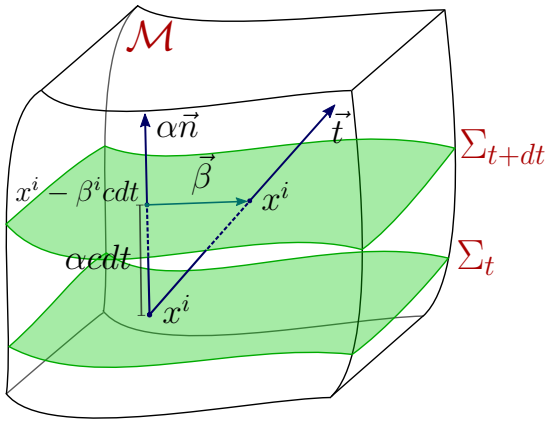

Figure 3.1: Illustration of two hypersurfaces, one at Σ_t and the other after a lapse αcdt, both embedded in a manifold $\mathcal{M}$. The observers at $\alpha\vec{n}$ and $\vec{t}$ are displaced by the length of the vector $\vec{\beta}$.

The *lapse function* $\alpha(t, x^i)$ quantify the time interval between hypersurfaces. It also shows the effect of time dilation related to both observers. This function is intrinsically related to the unit quadrivector $\vec{n}$. Evidently, $\vec{n}$ is parallel to the gradient of the scalar

field $\mathfrak{t}$, such that

$$n^\mu \doteq -\alpha \nabla^\mu \mathfrak{t}\,, \tag{3.1}$$

where $\alpha \doteq (-\nabla_\mu \mathfrak{t}\, \nabla^\mu \mathfrak{t})^{-1/2}$ and the signal is a convention to qualify n^μ as timelike, thus $n_\mu n^\mu = -1$, and Σ_t as spacelike. The *shift vector* $\vec{\beta}(t, x^i)$ is a spacelike function that measures the shift between Eulerian and coordinate observers after a time lapse. By analogy, we can imagine two particles at rest towards each other. If a gravitational wave passes through them, their coordinate separation remains constant, $\xi^\mu \doteq (0, \vec{\xi})$, different from the physical coordinates, $l \doteq (-g_{ij}\, \xi^i\, \xi^j)^{1/2}$. The quadrivector $\vec{\beta}$ compute the shift of the physical coordinates as given by the following relations,

$$x^i(t + dt) = x^i(t) - \beta^i(t, x^i)\, cdt\,, \tag{3.2}$$

$$\therefore\ \beta^i = -\alpha\, (\vec{n} \cdot \vec{\nabla} x^i)\,. \tag{3.3}$$

The *time vector* $\vec{t}$ follows the coordinate observer according to

$$t^\mu = \alpha n^\mu + \beta^\mu\,, \tag{3.4}$$

such that $t^\mu \nabla_\mu \mathfrak{t} = 1$, which guarantee that t^μ cannot be tangent to Σ_t. To measure the proper distance on Σ_t we define the spatial line element as

$$dl^2 = \gamma_{ij}\, dx^i dx^j\,, \tag{3.5}$$

in which γ_{ij} is the *spatial metric*. We now can express the complete line element defined by the ADM formalism,

$$\boxed{ds^2 = -(\alpha^2 - \beta_i \beta^i)\, c^2 dt^2 + 2\beta_i\, cdt\, dx^i + \gamma_{ij}\, dx^i dx^j}\,, \tag{3.6}$$

where the metric tensor and its contravariant form is shown as

$$g_{\mu\nu} = \begin{pmatrix} -\alpha^2 + \beta_i\beta^i & \beta_i \\ \beta_j & \gamma_{ij} \end{pmatrix}, \quad g^{\mu\nu} = \alpha^{-2} \begin{pmatrix} -1 & \beta^i \\ \beta^j & \alpha^2\gamma^{ij} - \beta^i\beta^j \end{pmatrix}.$$

The spatial metric is related to $g_{\mu\nu}$ as a *projection tensor*,

$$\gamma_{\mu\nu} = g_{\mu\nu} + n_\mu n_\nu \,, \tag{3.7}$$

since $\gamma_{\mu\nu}\, n^\nu = 0$ and $\gamma_{\mu\nu}\, t^\nu = \beta_\mu$. Assuming the relation above, it is possible to express the covariant and contravariant structures of the vectors (t^μ, n^μ, β^μ) and the spatial metric $\gamma_{\mu\nu}$ as

$$n^\mu = \alpha^{-1} \begin{pmatrix} 1 \\ -\beta^i \end{pmatrix}, \quad n_\mu = \alpha \begin{pmatrix} -1 & \vec{0} \end{pmatrix},$$

$$\beta^\mu = \begin{pmatrix} 0 \\ \beta^i \end{pmatrix}, \qquad \beta_\mu = \gamma_{\mu\nu}\, \beta^\nu \,,$$

$$t^\mu = \begin{pmatrix} 1 \\ \vec{0} \end{pmatrix}, \qquad t_\mu = \begin{pmatrix} -\alpha^2 & \beta^i \end{pmatrix},$$

$$\gamma_{\mu\nu} = \begin{pmatrix} \beta_l\, \beta^l & \beta_i \\ \beta_j & \gamma_{ij} \end{pmatrix}, \quad \gamma^{\mu\nu} = \begin{pmatrix} 0 & 0 \\ 0 & \gamma^{ij} \end{pmatrix}.$$

The four-dimensional volume element can be written in terms of the determinant of the spatial metric as $\sqrt{-g} = \alpha\, \gamma^{1/2}$.

The choice of a metric will depend on how we want to model our system. The functions α and β^μ adjust the form of the metric (3.6) and also carry the information about the chosen coordinate system, for these reasons, they are known as *gauge functions*. The spatial metric $\gamma_{\mu\nu}$, however, is described by a dynamical equation that we can identify by considering the (contracted) Bianchi identity,

$$\partial_0 G^{\mu 0} = -\partial_i G^{\mu i} - \Gamma^{\mu}_{\sigma\nu}\, G^{\sigma\nu} - \Gamma^{\nu}_{\sigma\nu}\, G^{\mu\sigma}\,. \tag{3.8}$$

As already discussed in Section 2.2.1, the right-hand side of the relation above (in $\Gamma^{\sigma}_{\mu\nu}$ and G^{ij}) presents second-order of time derivative, $\partial_0^2\, g_{\mu\nu}$, characterising the metric dynimics. As a consequence, the left-hand side also has to contain the same order of derivative, $\partial_0 G^{\mu 0} \;\rightarrow\; \partial_0^2\, g_{\mu 0}$, but we find that $G^{\mu 0}$ present only the first-order of time derivative, $G_{\mu 0} \;\rightarrow\; \partial_0 g_{\mu 0}$. Any physical system that its mathematical description presents only first-order time derivative does not constitute a dynamical regime since for null "velocities" at the initial condition the system will not evolve. That is why the necessity of a second-order time derivative to also evolve elements "at rest". It means that, from ten independent fields composed in the Einstein equation, six of them are genuinely responsible for the dynamics of the metric, and correspond to the components of γ_{ij}. The remain fields are part of the constraint conditions that we will investigate.

3.2 The extrinsic curvature

To derive the spatial metric evolution equation, we need before define an essential *extrinsic* property of a Riemannian manifold. Firstly, *intrinsic* properties are those independent whether their measurements are done in a manifold or submanifold [34]. For instance, we may idealise a tiny two-dimensional insect that lives on a two-dimensional sheet of paper. Both, the insect and us (conventional three-dimensional human beings) will measure the same value for the line element between two points in the paper, *i.e.*, the length does not depend on if the paper/submanifold is embedded into a three-dimensional space/manifold. As a consequence, the metric tensor is a collection of intrinsic quantities, as well as the Riemann tensor – which is also known as the *intrinsic curvature* tensor.

On the other hand, extrinsic properties do depend on whether their measurements are done in a manifold or submanifold. For example, if we roll the sheet of paper in a cylinder, the curvature of the paper will arise to us, but not for the insect because

it is also two-dimensional. We say that this is an *extrinsic curvature*. The extrinsic curvature tensor $K_{\mu\nu}$ is then defined as the gradient of the normal vector n^μ when it is parallel transported along of a slice Σ_t (see Fig. 3.2),

$$K_{\mu\nu} \doteqdot -\gamma_\mu^{\ \sigma}\, \nabla_\sigma n_\nu \,. \tag{3.9}$$

In the equation above, we see that the gradient is projected into the hypersurface, which indicates that the extrinsic curvature is purely spatial, $n^\mu K_{\mu\nu} = 0$. By its definition, it is said that this tensor is the negative form of the spacelike *expansion tensor*, which is similarly found in the Raychaudhuri equation [35] – as a timelike tensor. In addition, we may write $K_{\mu\nu} = -(\nabla_\mu n_\nu + n_\mu\, a_\nu)$, where $a_\nu \doteqdot n^\sigma \nabla_\sigma n_\nu$ is the *proper acceleration*.

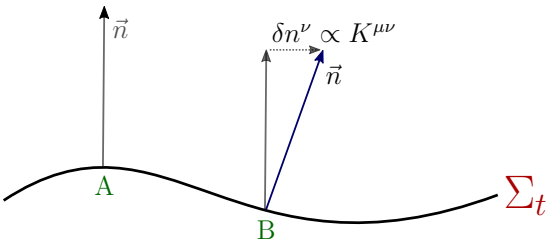

Figure 3.2: The normal vector $\vec{n}$ parallel transported from the point A to B on the hypersurface Σ_t. The variation of $\vec{n}$ in this process defines the measurement of the extrinsic curvature tensor $K_{\mu\nu}$.

The extrinsic curvature tensor may also be expressed in terms of the *Lie derivative* of the spatial metric $\gamma_{\mu\nu}$ along the flow of the normal vector $\vec{n}$. Since $n_\mu\, n^\mu = -1 \Rightarrow n^\nu \nabla_\mu n_\nu = 0$ and admitting Eq. (3.7), we obtain that,

$$\begin{aligned} \pounds_{\vec{n}} \gamma_{\mu\nu} &= n^\sigma \nabla_\sigma \gamma_{\mu\nu} + \gamma_{\mu\sigma} \nabla_\nu n^\sigma + \gamma_{\sigma\nu} \nabla_\mu n^\sigma = -2K_{\mu\nu} \,, \\ \therefore\ K_{\mu\nu} &= -\frac{1}{2} \pounds_{\vec{n}} \gamma_{\mu\nu} \,. \end{aligned} \tag{3.10}$$

For a given scalar field ϕ, we know that $\pounds_{\vec{n}} \gamma_{\mu\nu} = \phi^{-1} \pounds_{\phi\vec{n}} \gamma_{\mu\nu}$. From Eq. (3.4), $\pounds_{\vec{n}} = \alpha^{-1} \pounds_{\alpha\vec{n}} = \alpha^{-1}(\pounds_{\vec{t}} - \pounds_{\vec{\beta}})$, thereby we find the evolution equation for the spatial metric

in the following form,

$$\pounds_{\vec{t}}\gamma_{\mu\nu} = \pounds_{\vec{\beta}}\gamma_{\mu\nu} - 2\alpha K_{\mu\nu}\,. \tag{3.11}$$

To express this equation concerning the Lie derivatives is not useful for practical purposes once we have not chosen any aspect of the coordinate system. We, now, take advantage of the definition of the time vector $t^\mu = (1, \vec{0})$, which behaves as a *killing vector* since we may align it with the time component of the basis vector $\vec{e}_\mu$. Because $\vec{e}_0 \cdot \vec{\nabla}\mathfrak{t} = 1$, we can say that $\vec{t} = \vec{e}_0 = (1, \vec{0})$, and thus $\vec{e}_i$ is spacelike, $\vec{e}_i \cdot \vec{\nabla}\mathfrak{t} = 0$. In the *adapted coordinate system*, the Lie derivative with respect to $\vec{t}$ becomes,

$$\begin{aligned}\pounds_{\vec{t}}\gamma_{\mu\nu} &= \underbrace{t^{\sigma\nearrow 1}\partial_\sigma\gamma_{\mu\nu}}_{\sigma=0} + \underbrace{\gamma_{\mu\sigma}\partial_\nu t^{\sigma\nearrow 0} + \gamma_{\sigma\nu}\partial_\mu t^{\sigma\nearrow 0}}_{\vec{t}=\vec{e}_0} \\ &= \partial_0\gamma_{\mu\nu}\,.\end{aligned} \tag{3.12}$$

The covariant derivative ∇_μ was replaced by the partial form ∂_μ since the Lie derivative admits both structures whether the connection coefficients are symmetric. For the Lie derivative with respect to $\vec{\beta}$ we have that,

$$\begin{aligned}\pounds_{\vec{\beta}}\gamma_{\mu\nu} &= \beta^\sigma \nabla_\sigma \gamma_{\mu\nu}^{\nearrow 0} + \gamma_{\mu\sigma}\nabla_\nu\beta^\sigma + \gamma_{\sigma\nu}\nabla_\mu\beta^\sigma \\ &= D_\mu\beta_\nu + D_\nu\beta_\mu\,.\end{aligned} \tag{3.13}$$

where $D_\mu \doteqdot \gamma_\mu^{\ \nu}\nabla_\nu$ is the projected covariant derivative into the slice Σ_t. Substituting both Lie derivatives in Eq. (3.11), and since $\gamma_{\mu 0} = 0$, we obtain the evolution equation,

$$\boxed{\partial_0\gamma_{ij} = -2\alpha K_{ij} + D_i\beta_j + D_j\beta_i}\,. \tag{3.14}$$

These are six kinematic relations concerning to the lapse and shift functions – that depend on the gauge choices – and the extrinsic curvature, which also demands an evolution equation. Before we start to search for it, we need to derive two essential equations for integrability conditions. Another important expression for Eq. (3.14) is

its contracted form. Known that $\partial_\sigma \gamma = \gamma\, \gamma^{\mu\nu}\partial_\sigma \gamma_{\mu\nu}$, we get that

$$\boxed{\partial_0 \ln \gamma^{1/2} = -\alpha K + D_i \beta^i} \,. \tag{3.15}$$

3.3 Constraint equations

The evolution equation for the extrinsic curvature would have to present a relationship with the intrinsic curvature as a way to connect Einstein equation and get a 3+1 form of the GR. Initially, to project the intrinsic curvature tensor into the hypersurface Σ_t, we define the three-dimensional Riemann tensor as ${}^{(3)}R^{\sigma}{}_{\rho\mu\nu}\, v^\rho = 2D_{[\mu}D_{\nu]}v^\sigma$ for a given parallel transported vector v^σ. Computing the right-hand side of this expression,

$$\begin{aligned} D_\mu D_\nu v^\sigma &= D_\mu(\gamma_\nu{}^\alpha \gamma_\beta{}^\sigma \nabla_\alpha v^\beta) \\ &= \gamma_\mu{}^\kappa \gamma_\nu{}^\rho \gamma_\beta{}^\sigma (\nabla_\kappa \gamma_\rho{}^\alpha)(\nabla_\alpha v^\beta) + \gamma_\mu{}^\kappa \gamma_\nu{}^\alpha \gamma_\beta{}^\lambda (\nabla_\kappa \gamma_\lambda{}^\sigma)(\nabla_\alpha v^\beta) \\ &+ \gamma_\mu{}^\kappa \gamma_\nu{}^\alpha \gamma_\beta{}^\sigma (\nabla_\kappa \nabla_\alpha v^\beta)\,. \end{aligned} \tag{3.16}$$

Using Eq. (3.7) and $n_\mu \gamma_\nu{}^\mu = 0$ we find that $\gamma_\mu{}^\alpha \gamma_\nu{}^\beta \nabla_\alpha \gamma_\beta{}^\sigma = -n^\sigma K_{\mu\nu}$, and then, considering $n_\mu v^\mu = 0$ we get $K_{\mu\beta}\, n^\sigma \gamma_\nu{}^\alpha \nabla_\alpha v^\beta = K_\mu{}^\sigma K_{\nu\beta}\, v^\beta$. Substituting these terms in Eq. (3.16),

$$D_{[\mu}D_{\nu]}v^\sigma = \gamma_\mu{}^\kappa \gamma_\nu{}^\alpha \gamma_\beta{}^\sigma \nabla_{[\kappa}\nabla_{\alpha]}v^\beta - K^\sigma_{[\mu}K_{\nu]\beta}v^\beta \,, \tag{3.17}$$

known that $R^\sigma{}_{\rho\mu\nu}\, v^\rho = 2\nabla_{[\mu}\nabla_{\nu]}v^\sigma$ (the four-dimensional form), we finally obtain the *Gauss-Codazzi equation*,

$$\boxed{\gamma_\alpha{}^\sigma \gamma_\beta{}^\lambda \gamma_\mu{}^\kappa \gamma_\nu{}^\delta R_{\sigma\lambda\kappa\delta} = {}^{(3)}R_{\alpha\beta\mu\nu} + K_{\alpha\mu}K_{\beta\nu} - K_{\alpha\nu}K_{\mu\beta}} \,. \tag{3.18}$$

This equation describes the projection of the intrinsic curvature tensor into Σ_t related to the extrinsic curvature.

We can perform another projection of the Riemann tensor assuming the projected

covariant derivative of the extrinsic curvature tensor,

$$D_\mu K_{\nu\sigma} = -\gamma_\mu^{\ \alpha}\gamma_\nu^{\ \beta}\gamma_\sigma^{\ \kappa}\nabla_\alpha\nabla_\beta\, n_\kappa + K_{\mu\nu}\, a_\sigma\,. \tag{3.19}$$

Again, from the definition of the Riemann tensor, we write the *Codazzi-Mainardi equation*,

$$\boxed{\gamma_\alpha^{\ \delta}\gamma_\beta^{\ \kappa}\gamma_\mu^{\ \lambda}n^\nu R_{\delta\kappa\lambda\nu} = D_\beta K_{\alpha\mu} - D_\alpha K_{\beta\mu}}\,. \tag{3.20}$$

Both Eqs. (3.18) and (3.20) can be seen as integrability condition for projecting quantities from $(\mathcal{M},\, g_{\mu\nu})$ into $(\Sigma_t,\, \gamma_{ij})$. These equations are responsible for finding from Einstein equation its *constraints* – the $(\mu 0)$-fields.

Now, we will introduce a theory of gravity, the GR in astrophysical regime (which the cosmological constant *or* dark energy can be negligeble),

$$G_{\mu\nu} = \kappa\, T_{\mu\nu}\,. \tag{3.21}$$

We may find Einstein tensor as

$$\begin{aligned}\gamma^{\alpha\mu}\gamma^{\beta\nu}R_{\alpha\beta\mu\nu} &= R + n^\alpha n^\mu R_{\alpha\mu} + n^\beta n^\nu R_{\beta\nu} + n^\alpha \underbrace{n^\mu n^\nu n^\beta R_{\alpha\beta\mu\nu}}_{n^\nu\nabla_\mu n_\nu = 0} \\ &= 2n^\mu n^\nu G_{\mu\nu}\,.\end{aligned} \tag{3.22}$$

Contracting Eq. (3.18) twice, we write that

$$2n^\mu n^\nu G_{\mu\nu} = {}^{(3)}\!R + K^2 - K_{\mu\nu}K^{\mu\nu}\,, \tag{3.23}$$

where $K \doteqdot \gamma^{\mu\nu}K_{\mu\nu}$ is the *mean curvature* and ${}^{(3)}\!R \doteqdot \gamma^{ij}\,{}^{(3)}\!R_{ij}$ is the three-dimensional Ricci scalar, and ${}^{(3)}\!R_{ij}$ is expressed concerning the projected connection coefficients,

$${}^{(3)}\Gamma^i_{jk} = \tfrac{1}{2}\gamma^{il}\left(\partial_k\gamma_{lj} + \partial_j\gamma_{kl} - \partial_l\gamma_{jk}\right)\,, \tag{3.24}$$

such that ${}^{(3)}\Gamma^0_{\mu\nu} = 0$ since $\gamma^{0\lambda} = 0$. Assuming Eq. (3.21), we define that $c^2\rho \doteqdot n^\mu n^\nu T_{\mu\nu}$, and thus we get the *Hamiltonian constraint equation*,

$$\boxed{{}^{(3)}R + K^2 - K_{\mu\nu}K^{\mu\nu} = 2\kappa c^2\rho} \,. \tag{3.25}$$

A mixed contraction of the Einstein tensor can be described as $\gamma^{\alpha\mu}n^\nu G_{\mu\nu} = \gamma^{\alpha\mu}n^\nu R_{\mu\nu}$. Contracting Eq. (3.20), we obtain

$$\gamma^{\alpha\mu}n^\nu G_{\mu\nu} = D^\alpha K - D_\mu K^{\alpha\nu} \,. \tag{3.26}$$

Defining the *momentum density* $cj^\alpha \doteqdot -\gamma^{\alpha\mu}n^\nu T_{\mu\nu}$, we get the *momentum constraint equation*,

$$\boxed{D_\mu(K^{\alpha\mu} - K\gamma^{\alpha\mu}) = \kappa c j^\alpha} \,. \tag{3.27}$$

Equations (3.25) and (3.27) are responsive for the conservation of energy and momentum during the evolution of the system [36].

3.4 Evolution equations

Hitherto, we derived the evolution equation for the spatial metric (3.14) and got two constraints equations, the (00)-equation (3.25) and the (i0)-equation (3.27), given by Einstein equation (3.21). These steps were essential so that we can look for the evolution equation of the extrinsic curvature. Since the Lie derivative lets us describe the time derivative as in Eq. (3.11), we will apply the same procedure hereafter.

$$\begin{aligned}
\pounds_{\vec{n}} K_{\mu\nu} &= n^\alpha \nabla_\alpha K_{\mu\nu} + 2K_{\alpha(\mu}\nabla_{\nu)}n^\alpha \,; \quad (K_{\mu\nu} = -\nabla_\mu n_\nu - n_\mu a_\nu) \\
&= -[n^\alpha \nabla_\alpha \nabla_\mu n_\nu] - n^\alpha \nabla_\alpha (n_\mu a_\nu) - 2K_{\alpha(\mu}K^\alpha_{\nu)} - 2K_{\alpha(\mu}n_{\nu)}a^\alpha \\
&= -[R_{\lambda\nu\mu\alpha}n^\lambda n^\alpha + n^\alpha \nabla_\mu \nabla_\alpha n_\nu] - n^\alpha a_\nu \nabla_\alpha n_\mu - n^\alpha n_\mu \nabla_\alpha a_\nu
\end{aligned}$$

$$
\begin{aligned}
- \quad & 2K_{\alpha(\mu}K^{\alpha}_{\nu)} - 2K_{\alpha(\mu}n_{\nu)}a^{\alpha}\,; \quad (n^{\alpha}\nabla_{\mu}\nabla_{\alpha}n_{\nu} = \nabla_{\mu}a_{\nu} - K_{\mu}{}^{\alpha}K_{\alpha\nu} - n_{\mu}a^{\alpha}K_{\alpha\nu}) \qquad (3.28)\\
= \quad & -R_{\lambda\nu\mu\alpha}n^{\lambda}n^{\alpha} - \nabla_{\mu}a_{\nu} - a_{\mu}a_{\nu} - n^{\alpha}n_{\mu}\nabla_{\alpha}a_{\nu} - K_{\alpha\mu}K_{\nu}{}^{\alpha} - K_{\alpha\mu}n_{\nu}a^{\alpha}\,.
\end{aligned}
$$

The extrinsic curvature is a property of the space; such fact allows that $n^{\mu}\pounds_{\vec{n}}K_{\mu\nu} = 0$, and then the projection on the left-hand side of the equation above will remain the same,

$$
\begin{aligned}
\pounds_{\vec{n}}K_{\mu\nu} &= \gamma_{\mu}{}^{\sigma}\gamma_{\nu}{}^{\rho}\pounds_{\vec{n}}K_{\sigma\rho}\\
&= -\gamma_{\mu}{}^{\sigma}\gamma_{\nu}{}^{\rho}n^{\lambda}n^{\alpha}R_{\lambda\rho\sigma\alpha} - \gamma_{\mu}{}^{\sigma}\gamma_{\nu}{}^{\rho}\nabla_{\sigma}a_{\rho} - a_{\mu}a_{\nu} - K_{\alpha\mu}K_{\nu}{}^{\alpha}\,. \qquad (3.29)
\end{aligned}
$$

The proper acceleration can be related to the lapse function as

$$
\begin{aligned}
a_{\nu} &= n^{\mu}\nabla_{\mu}n_{\nu}\,; \quad (n_{\mu} = -\alpha\nabla_{\mu}\mathrm{t})\\
&= -n^{\mu}\nabla_{\mu}\alpha\,\nabla_{\nu}\mathrm{t} - \alpha\, n^{\mu}\nabla_{\mu}\nabla_{\nu}\mathrm{t}\\
&= D_{\nu}\ln\alpha\,, \qquad (3.30)\\
\therefore\ D_{\mu}a_{\nu} &= -a_{\mu}a_{\nu} + \alpha^{-1}D_{\mu}D_{\nu}\alpha\,. \qquad (3.31)
\end{aligned}
$$

Replacing the last expression in Eq. (3.29) we obtain the *Ricci equation*,

$$
\boxed{\pounds_{\vec{n}}K_{\mu\nu} = \gamma_{\mu}{}^{\sigma}\gamma_{\nu}{}^{\rho}n^{\lambda}n^{\delta}R_{\sigma\rho\lambda\delta} - \alpha^{-1}D_{\mu}D_{\nu}\alpha - K_{\sigma\mu}K_{\nu}{}^{\sigma}}\,, \qquad (3.32)
$$

which is a form for the dynamical equation of the extrinsic curvature independent of a geometrical gravitational theory. To introduce GR, we will use the contracted Eq. (3.18),

$$
\gamma^{\kappa\sigma}\gamma_{\beta}{}^{\lambda}\gamma_{\nu}{}^{\delta}R_{\sigma\lambda\kappa\delta} = {}^{(3)}R_{\beta\nu} + KK_{\beta\nu} - K_{\nu}{}^{\mu}K_{\mu\beta}\,. \qquad (3.33)
$$

Assuming Eq. (3.7) to evaluate $\gamma^{\kappa\sigma}$ on the left-hand side of the expression above, we rewrite and substitute it in the Ricci equation

$$
\pounds_{\vec{n}}K_{\mu\nu} = -\gamma_{\mu}{}^{\sigma}\gamma_{\nu}{}^{\rho}R_{\sigma\rho} + {}^{(3)}R_{\mu\nu} + KK_{\mu\nu} - 2K_{\sigma\mu}K_{\nu}{}^{\sigma} - \alpha^{-1}D_{\mu}D_{\nu}\alpha\,. \qquad (3.34)
$$

Considering the projected Einstein equation,

$$\gamma_\mu{}^\sigma \gamma_\nu{}^\rho R_{\sigma\rho} = \kappa \left(\gamma_\mu{}^\sigma \gamma_\nu{}^\rho T_{\sigma\rho} - \tfrac{1}{2} T \, \gamma_\mu{}^\sigma \gamma_\nu{}^\rho \, g_{\sigma\rho} \right) , \tag{3.35}$$

where we define the energy-momentum quantities projected into the hypersurface as $S_{\mu\nu} \doteqdot \gamma_\mu{}^\sigma \gamma_\nu{}^\rho \, T_{\sigma\rho}$, $S \doteqdot \gamma^{\sigma\rho} T_{\sigma\rho}$ and so $T = (\gamma^{\sigma\rho} - n^\sigma n^\rho) \, T_{\sigma\rho} = S - c^2 \rho$. Taking all these definitions and inserting them into the equation above to rewrite Eq. (3.34) – handling the adapted coordinate system – we get the *ADM evolution equation*,

$$\boxed{\begin{aligned} \partial_0 K_{ij} &= \beta^l \partial_l K_{ij} + K_{il} \partial_j \beta^l + K_{lj} \partial_i \beta^l - D_i D_j \alpha \\ &+ \alpha \left({}^{(3)}R_{ij} + K K_{ij} - 2 K_{il} K_j{}^l \right) + \kappa \alpha \left[\tfrac{1}{2} (S - c^2 \rho) - S_{ij} \right] \end{aligned}} . \tag{3.36}$$

Note that the first three terms on the right-hand side are related to $\pounds_{\vec{\beta}} K_{ij}$, and after that, we have the contribution of the lapse function, followed by the intrinsic and extrinsic curvature quantities in parentheses, and the last part is the source components. The contraction of this equation, replacing Eq. (3.25) and defining the projected Laplacian $D^2 \doteqdot \gamma^{ij} D_i D_j$, is given by

$$\boxed{\partial_0 K = \beta^i \partial_i K - D^2 \alpha + \alpha \left[K_{ij} K^{ij} + \tfrac{1}{2} \kappa \left(c^2 \rho + S \right) \right]} . \tag{3.37}$$

The evolution equations (3.14) and (3.36) are not in the original forms described by Arnowitt, Deser and Misner since they were looking for the Hamiltonian of the Einstein field equation. The dynamical equations were written concerning the spatial metric and the conjugate momenta regarding the Hamiltonian. This approach is addressed in the Appendix A.

Equations (3.14) and (3.36) together with the constraints (3.25) and (3.27) can be seen, by analogy, as the Maxwell equations, in which two of them are time-independent (the constraints), and the other two are time-dependent (dynamical equations). In electrodynamics, to solve this set of equations, we first study the physical system to

evaluate whether is necessary to introduce some gauge conditions – as the Coulomb gauge or the Lorentz gauge – and then, establish the boundary conditions – usually the Dirichlet or Neumann boundary conditions [37]. In the 3+1 formalism, these choices are the fundamental contributions of research in this area, what we will discuss in the next chapter.

3.5 Further analyses

In the Section 2.2.2, we reviewed some exact solutions of the Einstein field equation. Here, we will apply those metrics in 3+1 form in order to deepen our understanding of this formalism. Considering the Schwarzschild metric in radial isotropic coordinate,

$$ds^2 = -\left(\frac{1-r_s/4r}{1+r_s/4r}\right)^2 c^2dt^2 + \left(1+\frac{r_s}{4r}\right)^4 \eta_{ij}\, dx^i\, dx^j\,, \tag{3.38}$$

we compare with the ADM metric (3.6) and deduce that $\beta^i = 0$, $\alpha = \left(\frac{1-r_s/4r}{1+r_s/4r}\right)$ and $\gamma_{ij} = \left(1+\frac{r_s}{4r}\right)^4 \eta_{ij}$. Since the spatial metric is stationary, Eq. (3.14) tells us that in Schwarzschild spacetime there is no extrinsic curvature, $K_{ij} = 0$, and so, the spacetime does not evolve – which confirm the Birkhoff theorem. Once we are computing the field equations in a sourceless region, the constraints (3.25) and (3.27) vanish (on both sides of these equations).

From the previous analyses, we could note that for a system which presents extrinsic curvature the spatial metric should be time-dependent or carry the shift function (space-time terms). The Kerr spacetime has this last characteristic. Thereby, we will take into account the Kerr-Schild form,

$$ds^2 = -(1+\lambda\, l_0^2)c^2dt^2 - 2\lambda\, l_0\, l_i\, cdt\, dx^i + (\delta_{ij} - \lambda\, l_i\, l_j)dx^i dx^j\,. \tag{3.39}$$

This expression shows us $\beta^i = -\lambda\, l_0\, l^i$, $\alpha = (1+\lambda\, l_0^2)^{1/2}$ and $\gamma_{ij} = \delta_{ij} - \lambda\, l_i\, l_j$. Again, from Eq. (3.14), we take that $K_{ij} = (1+\lambda\, l_0^2)^{-1/2}\, \lambda^2\, l_0^2\, D_{(i}\, l_{j)}$. The projected covariant derivative, $D_i\, l_j$ is evaluated concerning the affine connections, that can be split into

3+1 form. Handling Eqs. (2.8) and (3.14) and known that $D_i\beta_j = \gamma^{-1/2}\,\partial_i\left(\gamma^{1/2}\,\beta_j\right)$, after some algebra we find the connections as following,

$$\Gamma^0_{00} = \alpha^{-1}\left(\partial_0\alpha + \beta^i\partial_i\alpha - \beta^i\beta^j K_{ij}\right), \tag{3.40}$$

$$\Gamma^0_{i0} = \alpha^{-1}\left(\partial_i\alpha - \beta^j K_{ij}\right), \tag{3.41}$$

$$\Gamma^0_{ij} = -\alpha^{-1}K_{ij}, \tag{3.42}$$

$$\Gamma^i_{00} = \alpha\,\partial^i\alpha - 2\alpha\beta^j K_j{}^i - \alpha^{-1}\beta^i\left(\partial_0\alpha + \beta^j\partial_j\alpha - \beta^j\beta^k K_{jk}\right) + \partial_0\beta^i + \beta^j\partial_j\beta^i, \tag{3.43}$$

$$\Gamma^i_{j0} = -\alpha^{-1}\beta^i\left(\partial_j\alpha - \beta^k K_{jk}\right) - \alpha K_j{}^i + D_j\beta^i, \tag{3.44}$$

$$\Gamma^i_{jk} = {}^{(3)}\Gamma^i_{jk} + \alpha^{-1}\beta^i K_{jk}. \tag{3.45}$$

Now, for a time-dependent spacetime, we will consider the FRW metric,

$$ds^2 = -c^2dt^2 + a(t)^2\eta_{ij}\,dx^i dx^j. \tag{3.46}$$

The lapse and shift functions become $\alpha = 1$ and $\beta^i = 0$. However, the spatial metric is related to the scale factor, $\gamma_{ij} = a^2\eta_{ij}$. As a consequence, the extrinsic curvature becomes $K_{ij} = -a\dot{a}\,\eta_{ij}$ and the mean curvature is $K = -3(\dot{a}/a)$, proportional to the Hubble factor ($H = \dot{a}/a$). As we already know that the cosmological field equations depend only on the scalar quantities, we compute Eqs. (3.25) and (3.37) to find, respectively, the Eqs. (2.24) and (2.25) – for $k = \Lambda = 0$.

Chapter 4

Gauges and inital conditions

In the previous chapter, we explore the reformulation of General Relativity in 3+1 spacetime. We got the set of equations from definitions established by the ADM formalism and took some analyses from well-known metrics. Here, we will investigate some implications of how the gauge choices affect our system description, as well as how to prepare our equations to receive initial conditions as the starting point to compute the dynamics.

The ADM formalism is described by the following set of equations.

$$
\begin{aligned}
ds^2 &= -(\alpha^2 - \beta_i\beta^i)\, c^2dt^2 + 2\beta_i\, cdt\, dx^i + \gamma_{ij}\, dx^i dx^j && (4.1)\\
& {}^{(3)}R + K^2 - K_{ij}K^{ij} = 2\kappa c^2\rho && (4.2)\\
& D_l(K^{il} - K\gamma^{il}) = \kappa c j^i && (4.3)\\
& \partial_0 \ln \gamma^{1/2} = -\alpha K + D_i\beta^i && (4.4)\\
\partial_0\gamma_{ij} &= -2\,\alpha K_{ij} + D_i\beta_j + D_j\beta_i && (4.5)\\
\partial_0 K &= \pounds_{\vec{\beta}}\, K - D^2\alpha + \alpha\left[K_{ij}K^{ij} + \tfrac{1}{2}\kappa\left(c^2\rho + S\right)\right] && (4.6)\\
\partial_0 K_{ij} &= \pounds_{\vec{\beta}}\, K_{ij} - D_iD_j\alpha + \alpha\left({}^{(3)}R_{ij} + KK_{ij} - 2K_{il}K_j{}^l\right) \\
&+ \kappa\alpha\left[\tfrac{1}{2}(S - c^2\rho) - S_{ij}\right] && (4.7)
\end{aligned}
$$

The source terms were defined as $c^2\rho = n^\mu n^\nu T_{\mu\nu}$, $cj^\sigma = -\gamma^{\sigma\mu}n^\nu T_{\mu\nu}$ and $S_{\sigma\rho} = \gamma_\sigma{}^\mu\gamma_\rho{}^\nu T_{\mu\nu}$.

In Numerical Relativity (NR), the research about gauges and initial condition meth-

ods are the main challenges in this area [38]. Many regimes can be adopted in NR, among them we have *critical collapse* (dust clusters [39, 40] and hydrodynamics [41, 42]), *high-energy collisions* (binary black hole [43, 44], binary neutron star [45, 46] and binary black hole-neutron star [47]), *gravitational waves* (compact objects [48, 49] and stochastic background [50, 51]), *alternative theory* (f(R) [52], Brans-Dicke [53] and scalar theory [54]) and *quantum gravity* (loop quantum gravity [55] and AdS theory [56]).

4.1 Initial conditions

The initial condition problem – also known as Cauchy problems – in 3+1 formalism means to set data about the gravitational fields (γ_{ij}, K_{ij}) ensuring the constraint equations. These quantities are regarding how a system can be described from a given instant of time. For instance, initial data can portray the following situation: we get a "photograph" of a black hole coalescence. In this picture, we have access to physical quantities, like their masses, spins, angular momenta, the distance toward each other and so forth. Then, a colleague could ask us: after a given time interval, how would be the next photo? In 3+1 form, we translate to: after taken all characteristics of the metric and curvature at that slice Σ_0, how would be the next slice after a time lapse? The procedures to evaluate our set of equations will be studied throughout this chapter.

4.1.1 Conformal transformations

The conformal transformation of the metric is an approach to rescale spacetime concerning a scalar field, $\tilde{g}_{\mu\nu} = \Psi(x^\sigma)\, g_{\mu\nu}$, which carry information about the curvature and symmetry at the initial condition [57]. Thus, we define the *conformal spatial metric* as

$$\tilde{\gamma}_{ij} \doteqdot \psi^{-4}\, \gamma_{ij}\,, \tag{4.8}$$

where $\psi(t, x^i)$ is the *conformal factor*. If we assume the determinant $\tilde{\gamma} \doteqdot 1$ we get that $\psi^4 = \gamma^{1/3}$, according to the identity $\partial_k \gamma = \gamma\gamma^{ij}\partial_k \gamma_{ij}$. Writing the conformal spatial

metric as $\tilde{\gamma}_{ij} = \gamma^{-1/3}\gamma_{ij}$, we identify $\tilde{\gamma}_{ij}$ as a *density tensor*[1] of weight $w = -2/3$ [58].

From the expression (4.8), we now can reformulate the whole geometrical quantities in conformal form [59]. The three-dimensional connection coefficients become

$$^{(3)}\Gamma^{i}_{jk} = \tilde{\Gamma}^{i}_{jk} + C^{i}_{jk}\,, \tag{4.9}$$

such that the conformal form of Eq. (3.24) is

$$\tilde{\Gamma}^{i}_{jk} = \frac{1}{2}\tilde{\gamma}^{il}\left(\partial_k\tilde{\gamma}_{lj} + \partial_j\tilde{\gamma}_{kl} - \partial_l\tilde{\gamma}_{jk}\right)\,. \tag{4.10}$$

The notation $^{(3)}$ will be omitted for conformal quantities since they all are related to the three-dimensional hypersurface. The *conformal tensor* C^{i}_{jk} is given by

$$\begin{aligned} C^{i}_{jk} &= \frac{1}{2}\gamma^{il}\left(\tilde{D}_k\gamma_{lj} + \tilde{D}_j\gamma_{kl} - \tilde{D}_l\gamma_{jk}\right)\,, \\ &= 2\left(\delta^{i}_{j}\tilde{D}_k\ln\psi + \delta^{i}_{k}\tilde{D}_j\ln\psi - \tilde{\gamma}_{jk}\tilde{D}^{i}\ln\psi\right)\,, \end{aligned} \tag{4.11}$$

and the conformal (projected) covariant derivative is defined as $\tilde{D}_i \doteqdot \tilde{\gamma}_i{}^{j}\nabla_j$, that is operated as the usual covariant derivative, *i.e.*, from a given vector v^i, we have that $D_j v^i = \tilde{D}_j v^i + C^{i}_{jk}v^k$.

The conformal Ricci tensor is found according to $2\tilde{D}_{[i}\,\tilde{D}_{j]}\,v^j = \tilde{R}_{ij}\,v^j$,

$$^{(3)}R_{ij} \doteqdot \tilde{R}_{ij} + R^{\psi}_{ij}\,, \tag{4.12}$$

$$\tilde{R}_{ij} = \partial_k\tilde{\Gamma}^{k}_{ij} - \partial_j\tilde{\Gamma}^{k}_{ik} + \tilde{\Gamma}^{l}_{ij}\tilde{\Gamma}^{k}_{lk} - \tilde{\Gamma}^{l}_{ik}\tilde{\Gamma}^{k}_{lj}\,, \tag{4.13}$$

$$\begin{aligned} R^{\psi}_{ij} &= \tilde{D}_k C^{k}_{ij} - \tilde{D}_j C^{k}_{ik} + C^{l}_{ij}\,C^{k}_{lk} - C^{l}_{ik}\,C^{k}_{lj} \\ &= -2\tilde{D}_i\tilde{D}_j\ln\psi + 4\tilde{D}_i\ln\psi\tilde{D}_j\ln\psi - 2\tilde{\gamma}_{ij}\tilde{D}_k\tilde{D}^{k}\ln\psi \\ &- 4\tilde{\gamma}_{ij}\tilde{D}_k\ln\psi\tilde{D}^{k}\ln\psi\,. \end{aligned} \tag{4.14}$$

[1] A tensor density is described by the Jacobian determinant weight w under a change of coordinates, $\mathcal{T}'^{\mu}{}_{\nu} = J^{w}\dfrac{\partial x'^{\mu}}{\partial x^{\sigma}}\dfrac{\partial x^{\rho}}{\partial x'^{\nu}}T^{\sigma}{}_{\rho}$; $J = \det\left(\dfrac{\partial x^{\mu}}{\partial x'^{\nu}}\right)$. In terms of the determinant of the metric, we simplify to $\mathcal{T}^{\mu}_{\nu} = g^{w/2}\,T^{\mu}_{\nu}$. The Lie derivative of a density tensor with respect to a vector $\vec{v}$ is then given by $\pounds_{\vec{v}}\mathcal{T}^{\mu}_{\nu} = ([\,v,\mathcal{T}\,]^{\mu}{}_{\nu})_{w=0} + w\,\mathcal{T}^{\mu}_{\nu}\partial_\sigma v^{\sigma}$.

From Eq. (4.12) the three-dimensional Ricci scalar becomes

$$\begin{aligned} {}^{(3)}R &= \psi^{-4}\,\tilde{\gamma}^{ij}\left(\tilde{R}_{ij} + R^{\psi}_{ij}\right) \\ &= \psi^{-4}\tilde{R} - 8\,\psi^{-5}\tilde{D}^2\psi\,. \end{aligned} \tag{4.15}$$

To obtain a conformal version of the extrinsic curvature tensor, we first need to decompose it into its trace K and the traceless part A_{ij},

$$K_{ij} = A_{ij} + \frac{1}{3}K\gamma_{ij}\,. \tag{4.16}$$

As well as the conformal spatial metric, $\tilde{A}_{ij}$ will transform to an arbitrary choice of the power of ψ – in that case, we got ψ^{-4} because the definition $\tilde{\gamma} = 1$. Our choice will depend on the divergent of A_{ij}, that appears in the constraint (4.3),

$$\begin{aligned} D_j A^{ij} &= \tilde{D}_i A^{ij} + C^{i}_{\ jk}A^{jk} + C^{j}_{\ jk}A^{ik}\,; \quad (C^{j}_{\ jk} = 6\tilde{D}_k \ln\psi) \\ &= \tilde{D}_j A^{ij} + 10A^{ik}\tilde{D}_k \ln\psi\,; \quad (\tilde{\gamma}_{jk}A^{jk} = 0 \;\rightarrow\; traceless) \\ &= \psi^{-10}\tilde{D}_j\left(\psi^{10}A^{ij}\right)\,, \end{aligned} \tag{4.17}$$

then, we define $\tilde{A}^{ij} \doteqdot \psi^{10}A^{ij}$, in which its covariant form is $\tilde{A}_{ij} = \psi^{-2}A_{ij}$. If we assume the field K as invariant under conformal transformation, $K = \tilde{K}$, the momentum constraint equation (4.3) becomes

$$\boxed{\tilde{D}_j\tilde{A}^{ij} - \frac{2}{3}\psi^6\tilde{\gamma}^{ij}\tilde{D}_j K = \kappa\,\psi^{10}cj^i}\,. \tag{4.18}$$

From the constraint (4.2) and using Eq. (4.15), the conformal Hamiltonian constraint is then given by

$$\boxed{8\tilde{D}^2\psi - \psi\tilde{R} - \frac{2}{3}\psi^5 K^2 + \psi^{-7}\tilde{A}_{ij}\tilde{A}^{ij} = -2\kappa\,\psi^5 c^2\rho}\,. \tag{4.19}$$

The initial conditions will depend on how we define a given set of fields at Σ_0.

Hereafter, we will explore some procedures that will allow us to evaluate correctly particular cases.

4.1.2 Conformal transverse-traceless (CTT) decomposition

The transverse-traceless (TT) decomposition is a technique to explore the tensor symmetries which simplify the mathematical description of it. As an illustration, the solution for the linearised Einstein equation,

$$\Box h^{\mu\nu} = -2\kappa\, T^{\mu\nu}\,, \tag{4.20}$$

where $g_{\mu\nu} = \eta_{\mu\nu} + h_{\mu\nu}$ ($h_{\mu\nu} \ll 1$) and $x^\mu \to x^\mu + \xi^\mu$, is given by

$$h^{\mu\nu} = C^{\mu\nu} \exp(i\, k_\sigma x^\sigma)\,. \tag{4.21}$$

The tensor $C^{\mu\nu}$ is responsible for the gravitational wave amplitude, and k^μ is the four-wavevector, such that $C^{\mu\nu}k_\nu = 0$. If we assume the propagation direction as $k^\mu = (k, 0, 0, k)$ and $\Box\xi^\mu = 0$ (that satisfy the Lorenz gauge, $\partial_\mu h^{\mu\nu} = 0$), the amplitude tensor becomes transverse and traceless,

$$C^{\mu\nu}_{TT} = \begin{pmatrix} 0 & 0 & 0 & 0 \\ 0 & a & b & 0 \\ 0 & b & -a & 0 \\ 0 & 0 & 0 & 0 \end{pmatrix}.$$

In short, $C^{\mu\nu}_{TT}$ is *transverse* once the wave propagation is transversal in k^3-direction (the longitudinal components become null) and *traceless* since the Lorenz gauge leads to $\Box\xi^\mu = 0$ [60].

Now that we get a concise comprehension of this approach, we will split our symmetric and traceless tensor $\tilde{A}^{ij}$ into its transverse-traceless $\tilde{A}^{ij}_{TT}$ and longitudinal form $\tilde{A}^{ij}_{L}$,

$$\tilde{A}^{ij} = \tilde{A}^{ij}_{TT} + \tilde{A}^{ij}_{L}\,, \tag{4.22}$$

in which, similar to the Helmholtz decomposition, they obey the expressions

$$\tilde{D}_j \tilde{A}^{ij}_{TT} = 0\,, \tag{4.23}$$

$$\tilde{A}^{ij}_{L} \doteq (\tilde{L}W)^{ij} = \tilde{D}^i W^j + \tilde{D}^j W^i - \frac{2}{3}\tilde{\gamma}^{ij}\tilde{D}_k W^k\,. \tag{4.24}$$

The vector W^i is an arbitrary vector-potential and $\tilde{L}$ is the *longitudinal operator* – or vector gradient. To reformulate Eq. (4.18), we have to compute the divergent of $\tilde{A}^{ij}$,

$$\begin{aligned}
\tilde{D}_j \tilde{A}^{ij} &= \tilde{D}_j \tilde{A}^{ij}_{L} = \tilde{D}_j (\tilde{L}W)^{ij} \doteq (\tilde{\Delta}_L W)^i\,; \quad (\tilde{D}_j \tilde{A}^{ij}_{TT} = 0) \\
&= \tilde{D}^2 W^i + \tilde{D}_j \tilde{D}^i W^j - \frac{2}{3}\tilde{D}^i \tilde{D}_j W^j\,; \quad (\tilde{R}^i{}_j v^j = \tilde{D}_j \tilde{D}^i v^j - \tilde{D}^i \tilde{D}_j v^j) \\
&= \tilde{D}^2 W^i + \frac{1}{3}\tilde{D}^i \tilde{D}_j W^j + \tilde{R}^i{}_j W^j\,,
\end{aligned} \tag{4.25}$$

in which $\tilde{\Delta}_L$ is the *vector Laplacian*. Thereby, the momentum constraint is written as

$$\boxed{(\tilde{\Delta}_L W)^i - \frac{2}{3}\psi^6 \tilde{\gamma}^{ij}\tilde{D}_j K = \kappa \psi^{10} c j^i}\,. \tag{4.26}$$

From the constraints (4.19) and (4.18) we note that the CTT decomposition demands initial data for ($\tilde{\gamma}_{ij}$, K, $\tilde{A}^{ij}_{TT}$). This method allows splitting the degrees of freedom (d.o.f) of our dynamical fields – six for each tensor since they are symmetric – into independent components. The spatial metric γ_{ij} decomposes its d.o.f with one for ψ and five for $\tilde{\gamma}_{ij}$; likewise the extrinsic curvature K_{ij} presents one d.o.f in K, two in $\tilde{A}^{ij}_{TT}$ and the remaining three in $\tilde{A}^{ij}_{L}$.

4.1.3 Conformal Thin-Sandwich (CTS) decomposition

For an alternative decomposition, we will consider for initial conditions the evolution rate of the spatial metric. It means that the first two neighbouring hypersurfaces have to be described before we evolve the dynamical equations, and that is the reason of the name *conformal "thin-sandwich"* decomposition. Therefore, we will define the traceless

part of the time derivative of the spatial metric,

$$u_{ij} \doteq \gamma^{1/3}\,\partial_0\left(\gamma^{-1/3}\,\gamma_{ij}\right)\,. \tag{4.27}$$

Considering Eqs. (4.4) and (4.5), we may write it in an alternative form,

$$\begin{aligned} u_{ij} &= \partial_0\gamma_{ij} - \frac{1}{3}\gamma^{-1}\gamma_{ij}\,\partial_0\gamma\,, \\ &= -2\alpha\,A_{ij} + (L\beta)_{ij}\,. \end{aligned} \tag{4.28}$$

The conformal description, as discussed in the previous section, depends on our arbitrary choice of the conformal factor power number, thus we establish that

$$\begin{aligned} \tilde{u}_{ij} &\doteq \partial_0\tilde{\gamma}_{ij}\,, \\ &= \psi^{-4}(\partial_0\gamma_{ij} - 4\gamma_{ij}\,\partial_0\ln\psi)\,; \quad (\psi=\gamma^{1/12}) \\ &= \psi^{-4}\,\gamma^{1/3}\,\partial_0(\gamma^{-1/3}\,\gamma_{ij})\,, \\ &= \psi^{-4}\,u_{ij}\,. \end{aligned} \tag{4.29}$$

Substituting Eq. (4.28) into (4.29), we find a complete conformal expression for $\tilde{u}_{ij}$,

$$\tilde{u}_{ij} = -2\,\tilde{\alpha}\tilde{A}_{ij} + (L\beta)_{ij}\,, \tag{4.30}$$

such that the procedure leads to the following conformal transformations [61],

$$\tilde{\alpha} = \psi^{-6}\,\alpha\,, \tag{4.31}$$

$$\tilde{\beta}_i = \psi^{-4}\,\beta_i \;\rightarrow\; \tilde{\beta}^i = \beta^i\,, \tag{4.32}$$

$$\tilde{D}_i = D_i \;\rightarrow\; \tilde{D}^i = \psi^4 D^i\,, \tag{4.33}$$

$$(\tilde{L}\beta)_{ij} = \psi^{-4}\,(L\beta)_{ij} \;\rightarrow\; (\tilde{L}\beta)^{ij} = \psi^4\,(L\beta)^{ij}\,. \tag{4.34}$$

The CTS decomposition redefines the momentum constraint (4.18) when we express

$\tilde{A}^{ij}$ using Eq. (4.30),

$$\boxed{(\tilde{\Delta}_L\beta)^i - (\tilde{L}\beta)^{ij}\tilde{D}_j \ln\tilde{\alpha} = \tilde{\alpha}\tilde{D}_j(\tilde{\alpha}^{-1}\tilde{u}^{ij}) + \frac{4}{3}\tilde{\alpha}\,\psi^6\tilde{D}^i K + 2\kappa\,\tilde{\alpha}\,\psi^{10}cj^i} \quad . \tag{4.35}$$

The equation above requires initial data for the variables $(\tilde{\alpha}, K, \tilde{\gamma}_{ij}, \tilde{u}_{ij})$. Different from CTT, in CTS decomposition we need to specify initial data for the spatial metric at Σ_0 and Σ_{dt} to express $\tilde{u}_{ij}$. As a consequence, the lapse and shift functions – in Eq. (4.35) – are necessary to join both slices.

4.1.4 Extended CTS decomposition

For a given specific initial condition, in CTS decomposition, when we do not know how to define the lapse function at Σ_0, we may calculate $\dot{K}$ instead of α. The *"extended" CTS* decomposition requires setting information about the mean curvature in the first two slices [62]. A new extra expression is provided by computing

$$\begin{aligned}
\tilde{D}^2(\alpha\psi) &= \psi^5 D^2\alpha + \alpha\tilde{D}^2\psi\,; \quad (LHS\ of\ Eq.(4.19)\ and\ RHS\ of\ Eq.(4.6)) \\
&= -\psi^5\dot{K} + \psi^5\beta^i D_i K + \alpha\,\psi^5\left[K_{ij}K^{ij} + \frac{1}{2}\kappa(\rho+S)\right] \\
&+ \frac{1}{8}\alpha\,\psi\tilde{R} + \frac{1}{12}\alpha\,\psi^5 K^2 - \frac{1}{8}\alpha\,\psi^{-7}\tilde{A}_{ij}\tilde{A}^{ij} - \frac{1}{4}\kappa\,\alpha\,\psi^5\rho\,; \quad (K_{ij}K^{ij} = \psi^{-12}\tilde{A}_{ij}\tilde{A}^{ij} + \tfrac{1}{3}K^2)
\end{aligned}$$

$$\boxed{\begin{aligned}
\therefore\ \tilde{D}^2(\alpha\psi) &= \alpha\psi\left[\tfrac{7}{8}\psi^{-8}\tilde{A}_{ij}\tilde{A}^{ij} + \tfrac{5}{12}\psi^4K^2 + \tfrac{1}{8}\tilde{R} + \tfrac{1}{4}\kappa\,\psi^4(\rho+2S)\right] \\
&- \psi^5\dot{K} + \psi^5\beta^i\tilde{D}_i K
\end{aligned}} \quad . \tag{4.36}$$

This equation depends on initial data for the fields $(K,\ \dot{K},\ \tilde{\gamma}_{ij},\ \tilde{u}_{ij})$, such that $\tilde{A}_{ij}$ is given by Eq. (4.30) and Eq. (4.35) determines the $\beta^i(t, x^i)$. All these decomposition techniques reformulate the constraint equations according to the initial condition necessities. The constraints seem to be more sophisticated and hard to be evaluated; however, the *gauge conditions* for the lapse and shift functions will make our calculations more feasible.

4.2 Gauge conditions

The functions lapse $\alpha(t, x^i)$ and shift $\beta^i(t, x^i)$ carry the chosen coordinate system and information from a slice Σ_t to its next neighbour. The choice of a gauge will decouple these functions from the field $g_{00}(t, x^i)$ into expressions that can be regarding our set of 3+1 equations. These expressions usually hold symmetries and are feasible to implement singularity avoidance algorithms.

4.2.1 Geodesic slicing

The simplest gauge describes a system in which the coordinate observer is at rest. In this case, the time vector t^μ and the four-velocity u^μ are parallel to the normal vector n^μ, thus $\beta^i = 0$ and $a_\nu = n^\mu \nabla_\mu n_\nu = 0$. Since the proper acceleration is null, it is said that the observer is in free fall, and then (s)he is following a geodesic. In the *geodesic slicing gauge*, we set $\alpha = 1$ and $\beta^i = 0$, and the dynamical equations become,

$$\partial_0 \gamma_{ij} = -2\, K_{ij}\,, \tag{4.37}$$

$$\partial_0 K_{ij} = {}^{(3)}R_{ij} + K K_{ij} - 2K_{il}K_j^{\ l} + \kappa \left[\tfrac{1}{2}(S - c^2\rho) - S_{ij}\right]. \tag{4.38}$$

Both expressions depend only on the source terms and the curvatures into Σ_t. As an example, we may cite the FRW metric (2.23).

4.2.2 Maximal slicing

For a freely-falling observer, $a_\mu = 0$, that is collapsed into a centre of mass or singularity its surrounding is characterised as a *maximal slicing* – as the Schwarzschild spacetime (2.14). In this gauge, the gravitational source does not present expansion or contraction,

$K = -\nabla_\mu n^\mu = 0$, that is in agreement to the variation of the total volume,

$$\begin{aligned}
\delta V &= \int_\Sigma d^3x\, \delta\gamma^{1/2}\,; \quad (\delta\gamma^{1/2} = \tfrac{1}{2}\gamma^{1/2}\gamma^{ij}\delta\gamma_{ij}) \\
&= \tfrac{1}{2}\int_\Sigma d^3x\, \gamma^{1/2}\gamma^{ij}\delta\gamma_{ij}\,; \quad (\delta\gamma_{ij} = \pounds_{\vec{n}}\gamma_{ij}\,\delta\vec{n} = -2K_{ij}\,\delta\vec{n}) \\
&= -\int_\Sigma d^3x\, \gamma^{1/2}\overset{\blacktriangledown}{K}{}^0\delta\vec{n} \;=\; 0\,.
\end{aligned} \tag{4.39}$$

The necessary condition for δV to be null, in the previous expression, is the mean curvature vanishes, $K = 0$. We may define a *rotational tensor* as $\omega_{ij} \doteqdot -\nabla_{[i}\, n_{j]}$ and its trace $\omega \doteqdot \gamma^{ij}\omega_{ij}$. However, since K_{ij} is symmetric $\omega = 0$, which we conclude that our observer moves as an incompressible and irrotational fluid.

The maximal slicing gauge condition carries a remarkable application in singularity avoidance techniques. Considering the sourceless form of Eq. (4.6) and the constraint (4.2), we get that

$$\boxed{D^2\alpha = {}^{(3)}\!R\,\alpha}\,. \tag{4.40}$$

We can take a qualitative solution of the equation above, for the boundary of a given radius r_0, as following

$${}^{(3)}\!R = \begin{cases} R_0\,, & r < r_0 \\ 0\,, & r > r_0 \end{cases},$$

where R_0 is a constant. For $\lim\limits_{r\to\infty}\alpha = 1$ and known that $\left(\dfrac{d\alpha}{dr}\right)_{r=0} = 0$, we obtain the solution

$$\alpha = \begin{cases} \dfrac{1}{\cosh\bar{r}_0}\dfrac{\sinh\bar{r}}{\bar{r}}\,, & \bar{r} < \bar{r}_0 \\ \\ 1 + \dfrac{\tanh\bar{r}_0 - \bar{r}_0}{\bar{r}}\,, & \bar{r} \geq \bar{r}_0 \end{cases},$$

such that $\bar{r} = r\,R_0^{1/2}$ and $\bar{r}_0 = r_0\,R_0^{1/2}$ [63]. Thereby, the singularity avoidance arises for $\lim\limits_{\bar{r}\to 0}\alpha = 1/\cosh\bar{r}_0$, preventing what is known as the *collapse of the lapse*.

Another important application of the maximal slicing gauge is to set, at the black hole initial data, linear momentum $\vec{p}$ and spin $\vec{s}$. To do so, we bring Eq. (4.26) and

– from the Schwarzschild metric in isotropic coordinates (2.15) – consider $\tilde{\gamma}_{ij} = \eta_{ij}$ to obtain the *Bowen-York solution* [64],

$$(\tilde{\Delta}_L W)^i = \partial^2 W^i + \frac{1}{3}\partial^i \partial_j W^j = 0\,. \tag{4.41}$$

We now perform a scalar-vector decomposition in W^i as $W_i = V_i + \partial_i U$, and then, we assume the gauge

$$\partial^2 U = -\frac{1}{4}\partial_i V^i\,, \tag{4.42}$$

to find the Laplace equation

$$\partial^2 V_i = 0\,. \tag{4.43}$$

These last two equations admit the solutions $V^i = 0$ and $U = k_1 - k_2/r$ (k_1 and k_2 are constants). Thereby, the vector-potential is $W^i = k_2\, l^i/r^2$, where $l^i = x^i/r$ and $r = \sqrt{x^2+y^2+z^2}$ in Cartesian coordinates. Substituting this solution into expression (4.24), the extrinsic curvature traceless part becomes [65],

$$\tilde{A}^s_{ij} = \frac{6}{r^3}\, l_{(i}\,\epsilon_{j)km}\, s^k\, l^m\,. \tag{4.44}$$

On the other hand, we could take $U = 0$ and propose $V^i = -2\,p^i/r$. Since the vector-potential also admit the solution [66],

$$\begin{aligned} W_i &= \frac{7}{8}V_i - \frac{1}{8}(\partial_i U - x^j \partial_i V_j)\,, &(4.45)\\ &= -\frac{1}{4r}(7\,p^i + l^i\, l_j\, p^j)\,, &(4.46)\end{aligned}$$

we present the momentum components for initial data,

$$\tilde{A}^p_{ij} = \frac{3}{2r^2}[2\,p_{(i}\,l_{j)} - (\eta_{ij} - l_i\, l_j)\, p_k\, l^k]\,. \tag{4.47}$$

Both Eqs. (4.44) and (4.47) form a solution for N black holes initial data,

$$\boxed{\tilde{A}_{ij} = \frac{3}{2}\sum_q^N \frac{1}{r_q^2}\left\{2\,p^q_{(i}\,l^q_{j)} - (\eta_{ij} - l^q_i\,l^q_j)\,p^q_k\,l^k_q + \frac{4}{r}\,l^q_{(i}\,\epsilon_{j)km}\,s^k_q\,l^m_q\right\}}\,. \tag{4.48}$$

4.2.3 Harmonic coordinates

The harmonic coordinates are those in which the geodesic coordinates satisfy the Laplace/d'Alembert equation, $\Box\, x^\sigma = 0$. As a consequence, it requires that

$$\begin{aligned}\Box\, x^\sigma &= g^{\mu\nu}\left(\partial_\mu\partial_\nu x^\sigma - \Gamma^\rho_{\mu\nu}\,\partial_\rho x^\sigma\right)\,,\\ &= g^{\mu\nu}\left(\partial_\mu\delta^\sigma_\nu - \Gamma^\rho_{\mu\nu}\delta^\sigma_\rho\right)\,,\\ &= -g^{\mu\nu}\,\Gamma^\sigma_{\mu\nu} \;=\; 0\,.\end{aligned} \tag{4.49}$$

We now define the contracted connection coefficients as

$$\Gamma^\sigma \doteqdot g^{\mu\nu}\,\Gamma^\sigma_{\mu\nu} = \frac{-1}{\sqrt{-g}}\partial_\rho\left(\sqrt{-g}\,g^{\rho\sigma}\right)\,, \tag{4.50}$$

in which, for $\Gamma^\sigma = 0$, leads to the coupled equations for the lapse and shift functions in harmonic coordinates [67],

$$\left(\partial_0 - \beta^j\partial_j\right)\alpha \;=\; -\alpha^2 K\,, \tag{4.51}$$

$$\left(\partial_0 - \beta^j\partial_j\right)\beta^i \;=\; -\alpha^2\left(\gamma^{ij}\partial_j \ln\alpha + {}^{(3)}\Gamma^i\right)\,, \tag{4.52}$$

where ${}^{(3)}\Gamma^i \doteqdot \gamma^{jk}\,{}^{(3)}\Gamma^i_{jk}$.

To generalise this coordinate condition for a broader gauge, we may establish the *gauge source function* H^σ, such that $\Gamma^\sigma = H^\sigma$ [68]. Assuming the projected Ricci tensor and considering only the second-order derivatives in the connection derivative terms, we

have that

$$\begin{aligned} R_{\mu\nu} &= \tfrac{1}{2}g^{\sigma\rho}\left(\partial_\sigma\partial_\mu g_{\nu\rho} - \partial_\sigma\partial_\rho\gamma_{\mu\nu} - \partial_\nu\partial_\mu\gamma_{\sigma\rho} + \partial_\nu\partial_\rho\gamma_{\mu\sigma}\right) \\ &+ \Gamma^\rho_{\mu\nu}\,\Gamma^\sigma_{\rho\sigma} - \Gamma^\rho_{\mu\sigma}\,\Gamma^\sigma_{\rho\nu}\,. \end{aligned} \tag{4.53}$$

Substituting this expression and Eq. (4.50) into Eq. (2.9), for $\Lambda = 0$, we get that

$$\boxed{g^{\sigma\rho}\partial_\sigma\partial_\rho g_{\mu\nu} + 2\partial_{(\mu}g^{\sigma\rho}\partial_\sigma g_{\nu)\rho} + 2H_{(\mu,\nu)} - 2H_\rho\Gamma^\rho_{\mu\nu} + 2\Gamma^\sigma_{\nu\rho}\Gamma^\rho_{\mu\sigma} = -2\kappa\left(T_{\mu\nu} - \tfrac{1}{2}Tg_{\mu\nu}\right)} \,. \tag{4.54}$$

The equation above is the nonlinear Einstein wave equation. This approach proved successful in simulating binary black holes [69]. If we set $H^\sigma = 0$ and take just the second-order derivative out for $g_{\mu\nu} = \eta_{\mu\nu} + h_{\mu\nu}$, we recover the linearised form of Einstein equation (4.20).

It is important to highlight that expressions (4.51) and (4.52) provide coordinate evolution equations since the functions $\alpha(t, x^i)$ and $\beta(t, x^i)$ carry information about how the coordinate observer moves concerning to the Eulerian observer, *i.e.*, how both reference frame "see" each other. The ADM equation, for instance, will evolve regarding we establish both observers relationship. Thereby, when we declare the harmonic coordinate gauge – in this condition – we are *free* to describe the coordinate speed throughout the hypersurface or how the lapse and shift functions behave close to singularities. When we say "free" of choice, of course, we should be careful about the choice stability [70, 71].

The generalised form of the harmonic coordinate gauge, $\Gamma^\sigma = H^\sigma$, has shown good results [72]. In particular, the search for a well-behaved solution for Eq. (4.51) has led the following equation,

$$\boxed{\left(\partial_0 - \beta^j\partial_j\right)\alpha = -2\alpha K} \,, \tag{4.55}$$

in which, for $\beta^i = 0$ and considering Eq. (4.4), we can find the solution as $\alpha = 1 + \ln\gamma$ [73]. The choice of Eq. (4.55) is so-called *1+log slicing* gauge [74].

4.2.4 Minimal distortion

In CTS decomposition for initial conditions, we have defined the traceless components of the time derivative of the metric u_{ij}, as a way to avoid to set the conformal transverse-traceless part of the extrinsic curvature $\tilde{A}^{TT}_{ij}$ at Σ_0. In numerical simulations, nonetheless, this approach may be unstable for strong field regimes since u_{ij} would evolve rapidly. To solve this problem, we can impose the *minimal distortion gauge* to assure the least time evolution rate of the spatial metric [75].

As we have done in Eq. (4.22) we will decompose u_{ij} into its transverse-traceless and longitudinal parts,

$$u_{ij} = u^{TT}_{ij} + u^{L}_{ij}\,, \tag{4.56}$$

$$\therefore \quad D^j u^{TT}_{ij} = 0\,, \tag{4.57}$$

$$\therefore \quad u^{L}_{ij} \doteq (L\,v)^{ij} = D_i\,v_j + D_j\,v_i - \frac{2}{3}\gamma_{ij} D^k\,v_k\,; \quad (\tilde{\gamma}_{ij} = \gamma^{-1/3}\gamma_{ij})$$

$$= \gamma^{1/3}\,\pounds_{\vec{v}}\,\gamma_{ij}\,. \tag{4.58}$$

This gauge condition requires the isometry for the least distortion of the hypersurface, $\pounds_{\vec{v}}\,\gamma_{ij} = 0$, and then $D^j u_{ij} = 0$. From Eq. (4.30), we define that $D^j(L\,\beta)_{ij} \doteq (\Delta_L\,\beta)_i = 2D^j(\alpha\,A_{ij})$. Using Eq. (4.18), we obtain

$$\boxed{(\Delta_L\,\beta)^i = 2A^{ij}D_j\alpha + \frac{4}{3}\alpha\,\gamma^{ij}D_j K + 2\kappa\alpha\,cj^i}\,. \tag{4.59}$$

To minimise the spatial metric distortion, the expression above must be satisfied. This equation was already shown in CTS decomposition, considering the conformal transformation, it becomes Eq. (4.35).

4.2.5 Gamma gauges

A more sophisticated and accurate alternative form to express the minimal distortion gauge, we consider an isometry of the conformal spatial metric in which we demand that

$\partial_j \tilde{u}^{ij} = \partial_0(\partial_j \tilde{\gamma}^{ij}) = 0$, thereby, the gauge source function is given by

$$\tilde{\Gamma}^i = -\partial_j \tilde{\gamma}^{ij} \,, \tag{4.60}$$

since $\gamma \doteq 1$ and $\tilde{D}_i \tilde{\gamma}^{ij} = 0$.

The so-called *Gamma-freezing gauge*, then, admit $\partial_0 \tilde{\Gamma}^i = 0$ [76]. To compute this constraint, we assuming the conformal form of Eq. (4.5),

$$\partial_0 \, \tilde{\gamma}^{ij} = \pounds_{\vec{\beta}} \, \tilde{\gamma}^{ij} - 2 \, \alpha \tilde{A}^{ij} \,, \tag{4.61}$$

where it was considered the conformal transformation $\tilde{A}_{ij} \doteq \psi^{-4} A_{ij}$ for Eq. (4.61) to be explicitly independent of the conformal factor. It is worth remembering that $\tilde{\gamma}^{ij}$ is a density tensor of weight 2/3 and its Lie derivative is $\pounds_{\vec{\beta}} \, \tilde{\gamma}^{ij} = \beta^k \partial_k \tilde{\gamma}^{ij} - \tilde{\gamma}^{ik} \partial_k \beta^j - \tilde{\gamma}^{kj} \partial_k \beta^i + \frac{2}{3} \tilde{\gamma}^{ij} \partial_k \beta^k$. The Gamma-freezing condition is then

$$\begin{aligned}
\partial_0 \tilde{\Gamma}^i &= \partial_j (\partial_0 \tilde{\gamma}^{ij}) \,; \quad [Eq.\,(4.61)] && (4.62)\\
&= \tilde{\gamma}^{jk} \partial_j \partial_k \beta^i + \frac{1}{3} \tilde{\gamma}^{ij} \partial_j \partial_k \beta^k + \beta^j \partial_j \tilde{\Gamma}^i - \tilde{\Gamma}^j \partial_j \beta^i + \frac{2}{3} \tilde{\Gamma}^i \partial_j \beta^j \\
&- 2 \partial_j \alpha \tilde{A}^{ij} - 2 \alpha \partial_j \tilde{A}^{ij} \,; \quad [Eq.\,(4.18)\, and\, \tilde{D}_j \tilde{A}^{ij} = \partial_j \tilde{A}^{ij} + \tilde{\Gamma}^i_{jk} \tilde{A}^{jk} + \tilde{\Gamma}^j_{jk} \tilde{A}^{ik}] && (4.63)\\
&= \pounds_{\vec{\beta}} \, \tilde{\Gamma}^i + \tilde{\gamma}^{jk} \partial_j \partial_k \beta^i + \frac{1}{3} \tilde{\gamma}^{ij} \partial_j \partial_k \beta^k - 2 \tilde{A}^{ij} \partial_j \alpha \\
&+ 2\alpha \left(\tilde{\Gamma}^i_{jk} \tilde{A}^{jk} + 6 \tilde{A}^{ij} \partial_j \ln \psi - \frac{2}{3} \tilde{\gamma}^{ij} \partial_j K - \kappa \, \psi^4 c j^i \right) . && (4.64)
\end{aligned}$$

Equation (4.64) together with the constraint $\partial_0 \tilde{\Gamma}^i = 0$ give us a type of Poisson equation, the Laplacian of β^i and the source terms, as well as Eq. (4.35).

Further researches in attempt to find an evolution equation for the shift function gauge, likewise Eq. (4.52), change the "freezing" condition to include the time derivative of β^i as following,

$$\partial_0 \beta^i = k \, \partial_0 \tilde{\Gamma}^i \,, \tag{4.65}$$

to give rise the *Gamma-driver gauge*. After numerical analyses, this equation underwent

modifications to become a second-order time derivative equation [77, 78],

$$\boxed{\partial_0^2 \beta^i = k\, \partial_0 \tilde{\Gamma}^i - \eta\, \partial_0 \beta^i} \,. \tag{4.66}$$

The constants k and η will depend on the gravitational system to be simulated. In the literature, Eq. (4.66) is often written as two coupled first-order equations with additional advection terms ($\beta^i\, \partial_i$) [79, 80],

$$(\partial_0 - \beta^j\, \partial_j)\beta^i = k\, B^i \,, \tag{4.67}$$

$$(\partial_0 - \beta^j\, \partial_j) B^i = (\partial_0 - \beta^j\, \partial_j)\tilde{\Gamma}^i - \eta\, B^i \,. \tag{4.68}$$

4.3 The puncture method

In this method, we will explore conformal flatness approach – in particular, the Schwarzschild metric – as a treatment for the black hole initial condition. As we have already discussed, in isotropic coordinates the line element is given by

$$ds^2 = -\left(\frac{1 - r_s/4r}{1 + r_s/4r}\right)^2 c^2 dt^2 + \psi^4\, \eta_{ij}\, dx^i dx^j \,, \tag{4.69}$$

where the conformal factor is $\psi = 1 + r_s/4r$ and the conformal spatial metric simplify to $\tilde{\gamma}_{ij} = \eta_{ij}$. For Eq. (4.19), the source term vanishes as well as the conformal Ricci scalar (4.15). Assuming the maximal slicing gauge, $K = 0$, the Hamiltonian constraint is

$$\tilde{D}^2 \psi = 0 \,. \tag{4.70}$$

Since $\tilde{\gamma}_{ij}$ is conformally flat, the previous equation reduces to the Laplacian equation, $\nabla^2 \psi = 0$, which admit the solution $\psi = 1 + r_s/4r$.

We examined in Section 3.5, however, that Schwarzschild spacetime does not evolve once the extrinsic curvature remains null. Therefore, unless we add particles, fluid or even another black hole, we will not have a dynamical spacetime. For the last example,

a binary black hole system, we can take advantage of an approximation similar to the superposition principle used in Coulombic interactions. A $30M_\odot$ black hole deflects $\approx 1''$ the trajectory of a light ray that passes nearby of it – according to the deflection formula $\Delta\phi = 2r_s/b$ (where b is the impact parameter). We may note, then, the indirect measurement of the spacetime curvature is small though sufficient to produce extremal phenomena. If we consider two black holes far enough away from each other, such that the space between them is *asymptotically flat*, our solution may be given by

$$\boxed{\psi = 1 + \frac{G}{2c^2}\sum_i^N \frac{m_i}{|\vec{r} - \vec{r}_i|}}\,, \tag{4.71}$$

in which m_i and $\vec{r}_i$ are the masses and positions of N black holes initially at rest in each reference frame.

Equation (4.71) presents the black hole singularities at $\vec{r} = \vec{r}_i$, which numerically is seen as grid spots without valid information – known as *punctures* [81, 82]. This method, the *Brill-Lindquist (BL) initial data*, has been shown to be an accurate approach to *at rest* black holes. This solution is computed by using the method of image, in which the image is seen as another universe connected with the "real" universe by the throat of a wormhole. Since two black holes present two images, each one in a different universe – that is said a solution with no *isometric*/identical universes – we cannot use the Bowen-York solution (4.48) to insert momentum end spin at Σ_0.

As an alternative to moving and spinning black holes, a more general solution of Eq. (4.48) is given by,

$$\begin{aligned}\tilde{A}_{ij} &= \frac{3}{2}\sum_q^N \frac{1}{r_q^2}\Big\{2\,p^q_{(i}\,l^q_{j)} - (\eta_{ij} - l^q_i\,l^q_j)\,p^q_k\,l^k_q \\ &\pm \frac{r_s^2}{r_q^2}[2\,p^q_{(i}\,l^q_{j)} - (\eta_{ij} - 5\,l^q_i\,l^q_j)\,p^q_k\,l^k_q] + \frac{4}{r}\,l^q_{(i}\,\epsilon_{j)km}\,s^k_q\,l^m_q\Big\}\,.\end{aligned} \tag{4.72}$$

The $\pm$ signs are concerning to the momentum sign of the black hole images. To complete the initial data solution, we have to guarantee the mass-energy conservation, recalculat-

ing the conformal factor using Eq. (4.19),

$$\tilde{D}^2\psi + \frac{1}{8}\psi^{-7}\tilde{A}_{ij}\tilde{A}^{ij} = 0\,. \tag{4.73}$$

Another approach to achieve this system is the *Brandt-Brügmann puncture method* [83]. In their solution, we can use the extrinsic curvature traceless part as Eq. (4.48) instead of Eq. (4.72). However, the conformal factor solution becomes

$$\psi = \psi_{BL} + u\,, \tag{4.74}$$

where ψ_{BL} is the same solution as Eq. (4.71) and the field u obays the Hamiltonian constraint in the conformally flat space,

$$\nabla^2 u + \frac{1}{8}\psi^{-7}\tilde{A}_{ij}\tilde{A}^{ij} = 0\,. \tag{4.75}$$

To evolve the metric – during the numerical simulation – without the puncture interference, different methods were proposed in the literature. For instance, we may cite the *black hole excision* which is a technique for ignoring the calculation at the puncture. Since black holes are characterized by their horizons, and we are interested in the dynamics in their surround, there is no need to evolve the spacetime inside of them [84, 85]. On the other hand, there are some methods in which some equations are modified. In this case, from our set of equations, we may be factoring out the metric to isolate the punctures into the conformal factor, and then, find its evolution equation to carry the punctures (black holes) through the hypersurfaces. This mechanism is known as *puncture evolution method*, and the most reputed scheme is the *BSSN formulation*.

In this method, two papers were published regarding a specific conformal transformation. Their authours, Shibata and Nakamura in the first paper [86], and Baumgarte and Shapiro in the second one [87], form the name of this formulation. All them were inspired by Nakamura, Oohara and Kojima's publication [88], in which they present dynamical equations regarding conformal transformation. The BSSN formulation con-

siders to expess the conformal factor ψ as an exponential function of another scalar field, as $\psi \doteqdot e^{\phi}$. Therefore, the conformal spatial metric becomes

$$\tilde{\gamma}_{ij} = e^{-4\phi}\,\gamma_{ij}\,. \tag{4.76}$$

The next step, then, is to reform the ADM set of equations. Using the evolution equation of the spatial metric determinant (4.4), such that $\psi^{-4} = \gamma^{1/3}$ and thus $\gamma = e^{-12\phi}$, we obtain

$$\boxed{\partial_0\phi = \pounds_{\vec{\beta}}\,\phi - \frac{1}{6}\alpha K}\,, \tag{4.77}$$

where $\pounds_{\vec{\beta}}\,\phi = \beta^i\partial_i\phi + \frac{1}{6}\partial_i\beta^i$. This equation is responsible for the puncture translation across the hypersurface. For $\tilde{\gamma}_{ij}$ evolution equation, we will consider Eq. (4.61), that requires us, together with Eq. (4.77), the fields $(K,\,\tilde{A}_{ij})$. Here, we will take into account the conformal transformation of the extrinsic curvature traceless part as $\tilde{A}_{ij} = e^{-4\phi}A_{ij}$, likewise in Section 4.2.5, and also the conformal connection functions $\tilde{\Gamma}^i \doteqdot -\partial_j\tilde{\gamma}^{ij}$.

To compute the mean curvature, we assume Eq. (4.6) and the trace-traceless decomposition, such that $K_{ij}K^{ij} = \tilde{A}_{ij}\tilde{A}^{ij} + \frac{1}{3}K^2$ and $\gamma^{ij}A_{ij} = 0$,

$$\partial_0 K = \pounds_{\vec{\beta}}K - D^2\alpha + \alpha\left(\tilde{A}_{ij}\tilde{A}^{ij} + \frac{1}{3}K^2\right) + \frac{1}{2}\kappa\alpha\left(c^2\rho + S\right)\,. \tag{4.78}$$

Now, we can rewrite the ADM equation (4.7). The left-hand side $\partial_0 K_{ij} = \partial_0[e^{4\phi}(\tilde{A}_{ij} + \frac{1}{3}K\tilde{\gamma}_{ij})]$ demands Eqs. (4.77), (4.78) and (4.61), and the right-hand side must be traceless as well as $X_{ij} = X^{TF}_{ij} + \frac{1}{3}X\gamma_{ij}$, where "TF" indicates trace-free components. Thus, the evolution equation follows as

$$\begin{aligned}\partial_0\tilde{A}_{ij} &= \pounds_{\vec{\beta}}\,\tilde{A}_{ij} + \alpha\left(K\tilde{A}_{ij} - 2\tilde{A}_{ik}\,\tilde{A}^k{}_j\right)\\ &+ e^{-4\phi}\left\{-D_iD_j\alpha + \alpha^{(3)}R_{ij} + \frac{1}{2}\kappa\alpha\left[(S - c^2\rho)\gamma_{ij} - 2S_{ij}\right]\right\}^{TF}\,.\end{aligned} \tag{4.79}$$

The three-dimensional Ricci tensor is given by

$$^{(3)}R_{ij} = \tilde{R}_{ij} + R^{\phi}_{ij}\,, \tag{4.80}$$

where $\tilde{R}_{ij}$ is rewritten in terms of $\tilde{\Gamma}^i = \tilde{\gamma}^{jk}\tilde{\Gamma}^i_{jk}$ and R^{ϕ}_{ij} considers the rescaling $\psi = e^{\phi}$,

$$\begin{aligned}
\tilde{R}_{ij} &= -\frac{1}{2}\tilde{\gamma}^{kl}\partial_k\partial_l\tilde{\gamma}_{ij} + \tilde{\gamma}_{k(i}\,\partial_{j)}\tilde{\Gamma}^k + \tilde{\Gamma}^k\,\tilde{\Gamma}_{(ij)k} \\
&+ \tilde{\gamma}^{kl}\left(2\tilde{\Gamma}^m_{k(i}\,\tilde{\Gamma}_{j)ml} + \tilde{\Gamma}^m_{il}\,\tilde{\Gamma}_{(ij)k}\right)\,, \qquad (4.81)\\
R^{\phi}_{ij} &= -2\tilde{D}_i\tilde{D}_j\phi - 2\tilde{\gamma}_{ij}\tilde{D}^k\tilde{D}_k\phi + 4\tilde{D}_i\phi\,\tilde{D}_j\phi - 4\tilde{\gamma}_{ij}\tilde{D}^k\phi\,\tilde{D}_k\phi\,. \qquad (4.82)
\end{aligned}$$

Equation (4.81) presents a spatial derivative of the conformal connection functions. For numerical purpose, we would get more stability considering an evolution equation for $\tilde{\Gamma}^i$ (4.64) – where the momentum constraint is admitted,

$$\begin{aligned}
\partial_0\tilde{\Gamma}^i &= \pounds_{\vec{\beta}}\,\tilde{\Gamma}^i + \tilde{\gamma}^{jk}\partial_j\partial_k\beta^i + \frac{1}{3}\tilde{\gamma}^{ij}\partial_j\partial_k\beta^k - 2\tilde{A}^{ij}\partial_j\alpha \\
&+ 2\alpha\left(\tilde{\Gamma}^i_{jk}\tilde{A}^{jk} + 6\tilde{A}^{ij}\partial_j\phi - \frac{2}{3}\tilde{\gamma}^{ij}\partial_j K - \kappa\, e^{4\phi}cj^i\right)\,. \qquad (4.83)
\end{aligned}$$

In Numerical Relativity, the BSSN formulation has been shown accurate and stable for simulation in different spacetime initial data. The next chapter, we will apply this method to perform numerical experiments.

Chapter 5

Numerical Relativity

Throughout this dissertation, we study all base ingredients to portray the theoretical requirements of some gravitational systems. From the ADM formalism, we described the whole set of dynamical equations, constraints, gauge conditions and initial data. In this chapter, we will put into practice this study developing numerical experiments for given regimes, and show techniques of Numerical Relativity (NR) to implement our equations in a numerical code.

To transcribe our equations into finite difference form, the vectors and tensor components have to be evaluated – as scalar fields – in each gridpoint every timestep. These spatial points represent the discretised hypersurface, such that each of them is interspersed by the *gridspacing* Δx. From a grid to the next – as well as from Σ_t to Σ_{t+dt} – we define the *finite time interval* Δt, in which the finite proper time interval $\Delta\tau = \alpha\Delta t$ appraises the rate of time that passes in each referential at the gridpoints concerning the gravitational source. The next step is to define how to perform the differential operators of equations.

5.1 Numerical differentiation

In the ADM set of equations, we find two kinds of differential operators, the first-order time derivative ∂_0 and the Lie derivative with respect to the shift vector $\pounds_{\vec{\beta}}$ – which is composed by first-order spatial derivative ∂_i . The choice of how we evaluate

them in finite difference will determine the accuracy of our simulations. To begin the implementation, we discretise the spatial operators by defining a given scalar field $u(t, x^i)$ and performing a Taylor series expansion as follows

$$u_i^n(x_i + \Delta x) \doteqdot u_{i+1}^n = u_i^n(x_i) + \Delta x\,(\partial_x u_i^n) + \frac{1}{2}(\Delta x)^2\,(\partial_x^2\, u_i^n) + \mathcal{O}(\Delta x^3)\,, \tag{5.1}$$

in which the index n signals the current finite time interval, and i shows the gridpoint position through the total discrete length N ($i = 1,2,...,N$). Thereby, the position on the hypersurface is $x_i = i \cdot \Delta x$ and its total length is $L = N/\Delta x$.

We now may truncate the series in the second-order $\mathcal{O}(\Delta x^2)$ and subtract the expression with $u_i^n(x_i - \Delta x)$ to obtain

$$\partial_x u_i^n \simeq \frac{1}{2\Delta x}\left(u_{i+1}^n - u_{i-1}^n\right)\,. \tag{5.2}$$

With the same procedure, we can represent the second-order derivative as

$$\partial_x^2\, u_i^n \simeq \frac{1}{\Delta x^2}\left(u_{i+1}^n - u_i^n + u_{i-1}^n\right)\,, \tag{5.3}$$

$$\partial_x \partial_y u_{ij}^n \simeq \frac{1}{4\Delta x^2}\left(u_{i+1,j+1}^n - u_{i+1,j-1}^n - u_{i-1,j+1}^n + u_{i-1,j-1}^n\right)\,. \tag{5.4}$$

We must emphasise that higher order finite differencing scheme allow higher resolution and accuracy for simulations; however, it increases the computational cost. On the other hand, there are advective terms ($\beta^i\,\partial_i$) that require fourth-order scheme for a satisfactory precision.

$$\partial_x u_i^n \simeq \frac{1}{12\Delta x}\left(u_{i+3}^n - 6u_{i+2}^n + 18u_{i+1}^n - 10u_i^n - 3u_{i-1}^n\right)\,, \quad \beta^x > 0\,, \tag{5.5}$$

$$\partial_x u_i^n \simeq \frac{1}{12\Delta x}\left(3u_{i+1}^n + 10u_i^n - 18u_{i-1}^n + 6u_{i-2}^n - u_{i-3}^n\right)\,, \quad \beta^x < 0\,. \tag{5.6}$$

These terms work as the speed of the spatial displacement rate, which can be found in the Lie derivatives, the 1+log (4.55) and the Gamma-driver (4.68) gauges.

For the time finite differencing scheme, there are two usual methods to evaluate evolution equations, the *Runge-Kutta* (RK) and the *Crank-Nicholson* (CN) methods [89]. Both are equivalent in performance of second-order accuracy. Here, we will consider the CN method to represent the equation $\partial_0 u = \mathcal{S}(u)$ in the scheme

$$u_i^{n+1} = u_i^n + \Delta t \left[\mathcal{S}(u_i^{n+1}) + \mathcal{S}(u_i^n)\right] . \tag{5.7}$$

This scheme can be evaluated by using tridiagonal matrix techniques. However, as a simpler alternative, we will choose the *iterative Crank–Nicholson* (ICN) method shown as follows

$$\begin{aligned} v_i^1 &= u_i^n + \Delta t\, \mathcal{S}(u_i^n) , & (5.8)\\ v_i^a &= u_i^n + \frac{\Delta t}{2}\left[\mathcal{S}(u_i^n) + \mathcal{S}(v_i^{a-1})\right] , & (5.9)\\ u_i^{n+1} &= v_i^{(\mathcal{Q})} , & (5.10) \end{aligned}$$

where $a = 2, ..., \mathcal{Q}$ is the interaction index. For the number of interactions (temporal finite differencing order) $\mathcal{Q} = 3$, the ICN method hits the same accuracy as CN method [90, 91].

Although we increase the accuracy order of finite differencing schemes, for a non-linear coupled set of equations the numerical noise may reach high-frequency modes along timesteps. Thus, it is convenient to add *artificial dissipative terms* in the equations to prevent the accumulation of noises. These terms present higher order of accuracy than the finite differencing operators. The most common dissipation technique in NR literature is the *Kreiss-Oliger* dissipation [92], which we express as

$$\partial_0 u = \mathcal{S}(u) - \frac{\epsilon}{\Delta x}(-1)^{\mathcal{Q}} \Delta_k^{2\mathcal{Q}} u , \tag{5.11}$$

where ϵ is an adjustment constant, such that $0 < \epsilon \Delta t/\Delta x < 1/2^{2\mathcal{Q}-1}$, and $\Delta_k^{2\mathcal{Q}} \doteqdot (\Delta_k^+ \Delta_k^-)^{\mathcal{Q}}$ is the forward-backward differencing operator. This operator is built concern-

ing the binomial expansion coefficients, for instance,

$$\Delta_i^4 u = u_{i+2}^n - 4u_{i+1}^n + 6u_i^n - 4u_{i-1}^n + u_{i-2}^n\,, \quad (\mathcal{Q}=2) \tag{5.12}$$

$$\begin{aligned}\Delta_i^8 u &= u_{i+4}^n - 8u_{i+3}^n + 28u_{i+2}^n - 56u_{i+1}^n + 70u_i^n \\ &- 56u_{i-1}^n + 28u_{i-2}^n - 8u_{i-3}^n + u_{i-4}^n\,. \quad (\mathcal{Q}=4)\end{aligned} \tag{5.13}$$

5.2 Theoretical requirements

For numerical experiments, let us consider a binary black hole (BBH) system since the set of equations are simplified but evolve a non-trivial dynamical spacetime. The black hole mechanics is not an easy subject at all; however, its advantages are in calculate only the left-hand side of Einstein equation and avoid the need of hydrodynamic or geodesic equations. From the simulations, we will obtain the gravitational field components to visualise the black holes as punctures.

We will consider, for the metric components, the 1+log (4.55) and Gamma-driver (4.68) gauges to evolve the lapse and shift functions. The spatial metric will be rescaling by using the conformal factor, as a way to simplify the implementation of black holes initial data. In BSSN formulation, the punctures do not need excision techniques – that require algorithm modifications – on the other hand, we evolve them running an evolution equation (4.77). However, at the black holes positions, our set of equations diverge, $\psi \to \infty$, thereby we will redefine the conformal factor as $\chi \doteqdot \psi^{-4} = e^{-4\phi}$ for better numerical computation [93]. In χ-version, we find punctures at $\chi = 0$, and around them, this scalar field grows linear, what decreases the numerical instability. For terms with the inverse of χ, we set $\lim_{\chi\to 0} \chi^{-1} = 1/\sigma$ such that $\sigma < (2r_{min}/m)^4$, the approximate initial value of χ at a minimum distance r_{min} between the punctures [80]. A well-chosen value for σ will not interfere in the spacetime evolution, once we are only interested in analysing the physics outside the black hole horizons.

The new conformal factor rescaling changes the BSSN formulation such that $\partial_i\phi = -\frac{1}{4}\chi^{-1}\partial_i\chi$ and $\partial_i\partial_j\phi = \frac{1}{4}\chi^{-2}\partial_i\chi\partial_j\chi - \frac{1}{4}\chi^{-1}\partial_i\partial_j\chi$. Assuming the vacuum solution, $\rho = j^k = S_{ij} = 0$, we obtain a set of eight nonlinear coupled equations from $G_{\mu\nu} = 0$,

$$\begin{aligned}
\partial_t\chi &= \pounds_{\vec{\beta}}\,\chi + \tfrac{2}{3}\chi\left(\alpha K - \partial_i\beta^i\right), && (5.14)\\
\partial_t\alpha &= \pounds_{\vec{\beta}}\,\alpha - 2\alpha K, && (5.15)\\
\partial_t\tilde{\gamma}_{ij} &= \pounds_{\vec{\beta}}\,\tilde{\gamma}_{ij} - 2\alpha\tilde{A}_{ij}, && (5.16)\\
\partial_t K &= \pounds_{\vec{\beta}}\,K - D^2\alpha + \alpha\left(\tilde{A}_{ij}\tilde{A}^{ij} + \tfrac{1}{3}K^2\right), && (5.17)\\
\partial_t\tilde{\Gamma}^i &= \pounds_{\vec{\beta}}\,\tilde{\Gamma}^i + \tilde{\gamma}^{jk}\partial_j\partial_k\beta^i + \tfrac{1}{3}\tilde{\gamma}^{ij}\partial_j\partial_k\beta^k - 2\tilde{A}^{ij}\partial_j\alpha\\
&+ 2\alpha\left(\tilde{\Gamma}^i_{jk}\tilde{A}^{jk} - \tfrac{3}{2}\chi^{-1}\tilde{A}^{ij}\partial_j\chi - \tfrac{2}{3}\tilde{\gamma}^{ij}\partial_j K\right), && (5.18)\\
\partial_t B^i &= \beta^j\partial_j B^i - \eta B^i + (\partial_t - \beta^j\partial_j)\tilde{\Gamma}^i, && (5.19)\\
\partial_t\beta^i &= \beta^j\partial_j\beta^i + \tfrac{3}{4}B^i, && (5.20)\\
\partial_t\tilde{A}_{ij} &= \pounds_{\vec{\beta}}\,\tilde{A}_{ij} + \alpha\left(K\tilde{A}_{ij} - 2\tilde{A}_{ik}\,\tilde{A}^k{}_j\right)\\
&+ \chi\left(-D_iD_j\alpha + \alpha^{(3)}R_{ij}\right)^{TF}, && (5.21)
\end{aligned}$$

in which $\pounds_{\vec{\beta}}\chi = \beta^i\,\partial_i\chi$, whose weight is $w = 0$ as well as for α and K scalar fields. It is worth remembering that for density rank-1 tensor as $\tilde{\Gamma}^i$, $w = 2/3$; and density rank-2 tensors, $w = -2/3$. We consider the *geometrical units* ($c = G = 1$), since very large or very small physical constants may favour higher modes of numerical noise, thus $\partial_0 = \partial_t$.

The components of the three-dimensional Ricci tensor, ${}^{(3)}R_{ij} = \tilde{R}_{ij} + R^{\chi}_{ij}$, are rewritten in the form

$$\begin{aligned}
\tilde{R}_{ij} &= -\frac{1}{2}\tilde{\gamma}^{kl}\partial_k\partial_l\tilde{\gamma}_{ij} + \tilde{\gamma}_{k(i}\,\partial_{j)}\tilde{\Gamma}^k + \tilde{\Gamma}^k\,\tilde{\Gamma}_{(ij)k} + \tilde{\gamma}^{kl}\left(2\tilde{\Gamma}^m_{k(i}\,\tilde{\Gamma}_{j)ml} + \tilde{\Gamma}^m_{il}\,\tilde{\Gamma}_{(ij)k}\right), && (5.22)\\
R^{\chi}_{ij} &= \frac{1}{2\chi}\tilde{D}_i\tilde{D}_j\chi + \frac{1}{2\chi}\tilde{\gamma}_{ij}\tilde{D}^2\chi - \frac{1}{4\chi^2}\tilde{D}_i\chi\,\tilde{D}_j\chi - \frac{3}{4\chi^2}\tilde{\gamma}_{ij}\tilde{D}_k\tilde{D}^k\chi. && (5.23)
\end{aligned}$$

The structure of the spatial curvatures are recovered from the definitions $\tilde{\gamma}_{ij} = \chi\,\gamma_{ij}$ and $\tilde{A}_{ij} = \chi\left(K_{ij} - \frac{1}{3}K\gamma_{ij}\right)$.

5.3 Numerical experiments

After establishing the whole set of equations which will compute $G_{\mu\nu} = 0$ for a BBH system, we will now define the initial data and show the simulation results for two regimes. Both experiments, we consider two equal mass black holes of $M = 0.5$ positioned at a distance $d = 15\, r_s = 30M$ between them in a $(400M)^2$ grid. Since very long simulation time is not advantageous for this dissertation, we will choose to evolve a 2+1 spacetime. We will perform the slices along the time $T = 600M$.

In the first scenario, the initial data requires the geodesic slicing gauge ($\alpha = 1$, $\beta^i = 0$) combined with the maximal slicing condition, $K = 0$, discussed in Section 4.2. The conformal spatial metric admits the asymptotically flatness condition, $\tilde{\gamma}_{ij} = \eta_{ij}$, and the conformal factor $\chi = \psi^{-4}$ considers the Brill-Lindquist initial data (4.71),

$$\psi = 1 + \frac{M}{2}\left(\frac{1}{|\vec{r} - \vec{c}_1|} + \frac{1}{|\vec{r} - \vec{c}_2|}\right). \tag{5.24}$$

For static and spinless black holes, we set $\tilde{A}_{ij} = 0$ to simulate a *head-on* BBH collision. These initial conditions are summarised in Fig. 5.1, in which is shown the only non-null field, the conformal factor χ.

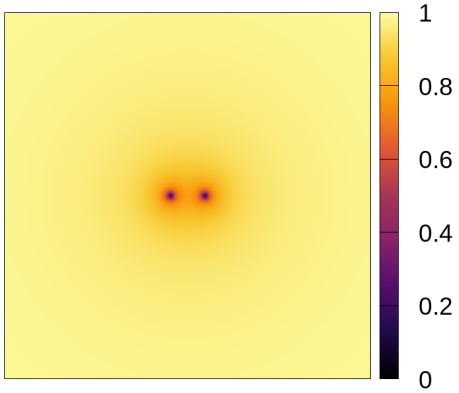

Figure 5.1: Snapshot of the conformal factor χ at Σ_0. The punctures are set considering the Brill-Lindquist initial data.

During the evolution of the equations, we fix the damping parameter $\eta = 1.5/M$ and the adjustement parameter, from Kreiss-Oliger dissipation method, $\epsilon = 10^{-3}$. In Fig. 5.2, it is shown the simulation snapshots of a head-on collision of two black holes, represented by the scalar fields (χ, K, $\tilde{\gamma}_{11}$, $\tilde{A}_{11}$) – from the top to the bottom – which

were chosen for better visualisation of the slice curvatures.

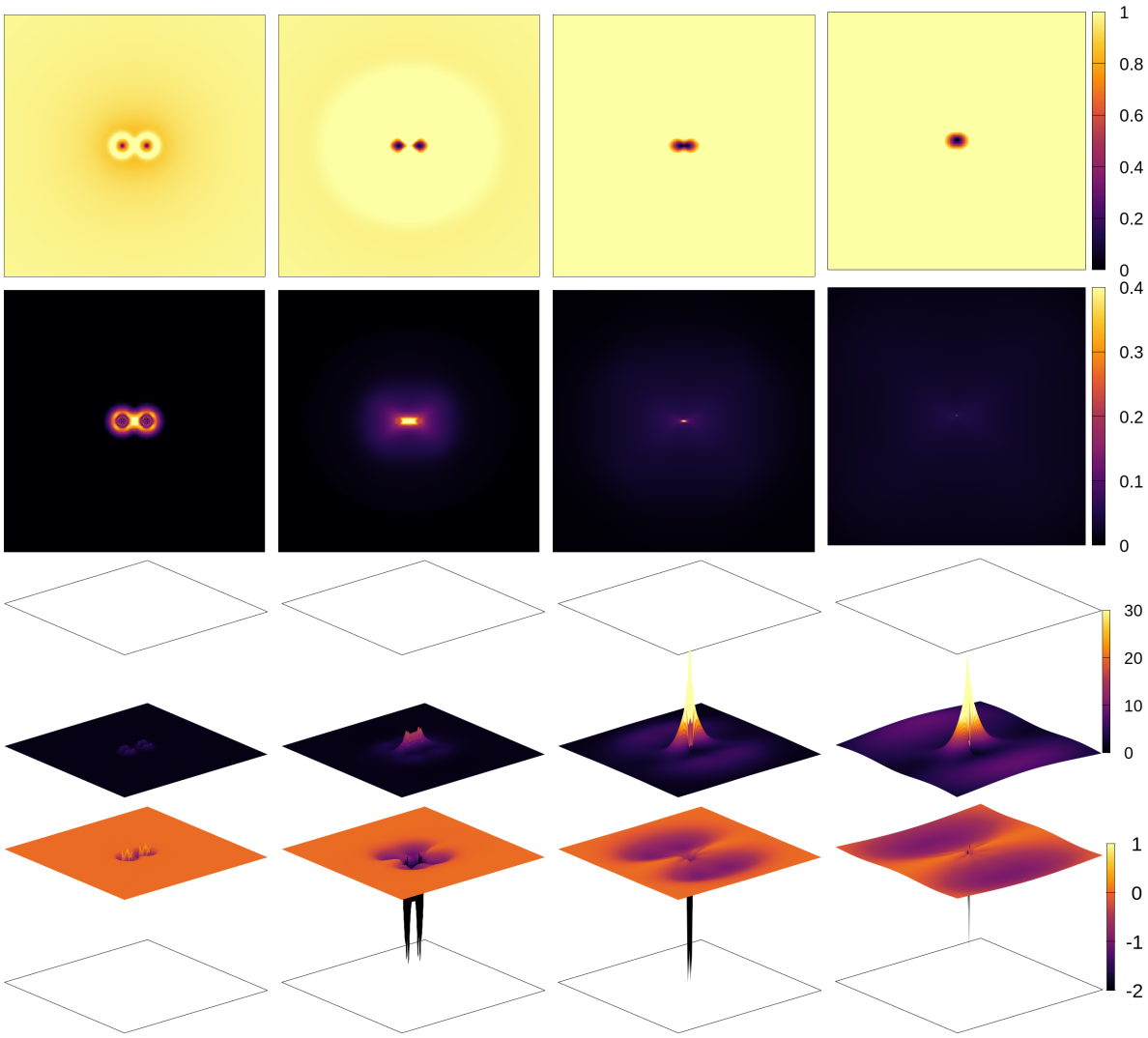

Figure 5.2: Snapshots of a head-on collision binary black hole simulated in a $L = 400M$ square grid over the time $T = 600M$. The sequence from the top to the bottom is showing the scalar fields χ, K, $\tilde{\gamma}_{11}$ and $\tilde{A}_{11}$. The sequence from left to right represents the time instants at $T = 30M$, $T = 160M$, $T = 400M$ and $T = 600M$.

From left to right we read the time flow, in which the first snapshots the black holes are gravitationally bound, they present linear momentum and spin. Once the shift evolution equation starts to evolve, the shift vector $\vec{\beta}$ increases and – from analyses of the Kerr metric – the black holes gain spin. The second snapshots the black holes are separated by a distance of about $6M$ that is measured from the expression $\partial_t \vec{x}_p = -\vec{\beta}(\vec{x}_p)$ at the punctures [93]. The third snapshots show the *plunge-merger* phase where the punctures form a peanut shape; the immediate point before them rapidly collapse into a unique singularity. The fourth snapshots are the final phase in which a resultant black

hole arises with the mass slightly smaller than the sum of the initial ones – since part of the total mass is spent into gravitational waves (GW)s energy. During the short instant of this last phase, the remaining puncture still oscillates in spheroidal shapes until it stabilises into a spherically symmetric form. These oscillations perturb the spacetime producing its last ripples in lower frequencies whose characteristics compose the so-called *ringdown* phase configuration.

The head-on numerical experiment provided to be stable even after the black holes collapse. This simulation reveals that the equations are correctly implemented once any mistake would violate the constraint equations and propagate high modes of numerical noise.

In the second numerical experiment, the initial data undergoes changes to add momentum and spin to form a *quasi-circular orbit* configuration. This initial step has to be solved with more accuracy since brusque adjustments of fields during the evolution may increase numerical noise. Therefore, we will modify the geodesic slicing gauge to calculate the lapse function as given by the isotropic Schwarzschild metric, $\alpha = (1 - r_s/4r)/(1 + r_s/4r) = 2\chi^{1/4} - 1$. However, for an even better approximation to the lapse evolution, we will set as initial data $\alpha \simeq \chi^{1/2}$.

At the slice Σ_0, the momentum and spin addition alter the spatial curvature which means that the tensor $\tilde{A}_{ij}$ is not "flat" in the whole slice, and then, we will require the Bowen-York initial data (4.48),

$$\tilde{A}_{ij} = \frac{3}{2}\sum_{q=1}^{2}\frac{1}{r_q^2}\left\{2\,p^q_{(i}\,l^q_{j)} - (\eta_{ij} - l^q_i\,l^q_j)\,p^q_k\,l^k_q + \frac{4}{r}\,l^q_{(i}\,\epsilon_{j)km}\,s^k_q\,l^m_q\right\}. \tag{5.25}$$

In Fig. 5.3, the $\tilde{A}_{ij}$ snapshot presents the curvature for a clockwise motion of the punctures, where they were set momenta $\vec{p}_1 = (-0.18, 0.0)$, $\vec{p}_2 = (0.18, 0.0)$, and spins $\vec{s}_1 = (-0.01, 0.0)$, $\vec{s}_2 = (0.01, 0.0)$.

To construct the conformal factor in these conditions, we need to consider the Brandt-Brügmann puncture method (4.74), $\psi = \psi_{BL} + u$, that guarantees the Hamiltonian constraint (4.75), $\nabla^2 u(\vec{x}) = S(u)$ for $S(u) = -\frac{1}{8}\psi^{-7}\tilde{A}_{ij}\tilde{A}^{ij}$. We may solve this constraint computing it in Fourier space, $\bar{u}(\vec{k}) = -k^{-2}\bar{S}(\vec{k})$.

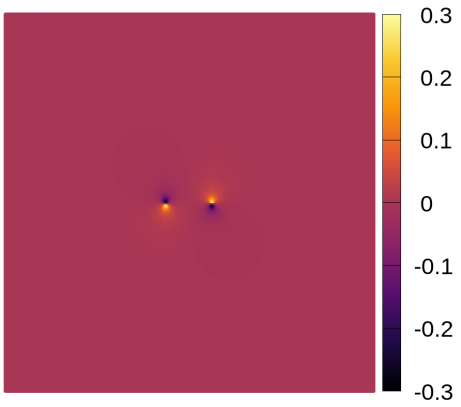

Figure 5.3: Snapshot of the conformal traceless part of the extrinsic curvature $\tilde{A}_{ij}$. The Bowen-York initial data produces the grid folds as a way to insert momentum and spin.

The result of the simulation is seen in Fig. 5.4, in which the punctures move in an ellipse of great eccentricity due to the low value of momentum magnitude. In the first snapshots the punctures – top to bottom – start a smooth spiral collapse into their centre of mass. The mean curvature K shows higher values in clockwise direction, as difined in $\tilde{A}_{ij}$ at Σ_0.

The second snapshots, the black holes separation is around $5M$, what is particularly interesting to study GWs emission. This distance is the turning point between stable and unstable circular orbit, and then, represent the equilibrium energy phase, known as the *innermost stable circular orbit* (ISCO) [94]. After r_{ISCO}, analytical approximations as the Post-Newtonian description does not prevent GW frequency correctly.

In the third snapshot series, the *plunge-merger* phase, the GW frequency reaches maximum values once the higher the velocity of collapse, the higher is the curvature amplitude, shown in the $\tilde{A}_{11}$ component of the conformal traceless part of the extrinsic curvature. This amplitude is also explicit in the mean curvature K, where a small point of high curvature displays the centre of mass.

The ringdown phase, the fourth snapshots – as well as the head-on collision – show a remaining puncture which oscillates in spheroidal shapes. However, in each experiment the ringdown GWs will present different modes of spherical harmonics, but both for short duration time due to the initial data imposed.

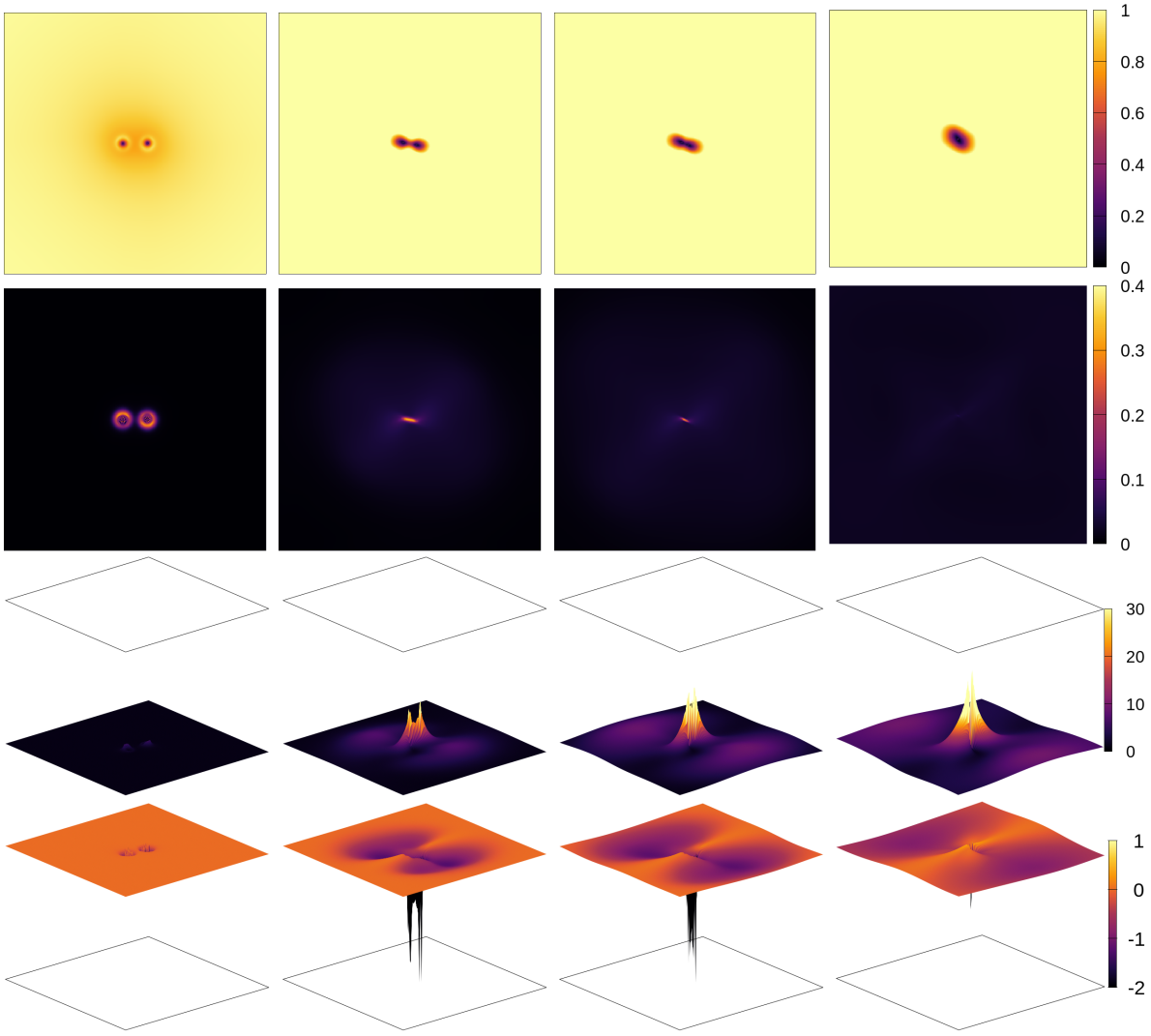

Figure 5.4: Snapshots of a smooth spiral coalescence binary black hole simulated in a $L = 400M$ square grid over the time $T = 600M$. The sequence from the top to the bottom is showing the scalar fields χ, K, $\tilde{\gamma}_{11}$ and $\tilde{A}_{11}$. The sequence from left to right represents the time instants at $T = 10M$, $T = 160M$, $T = 240M$ and $T = 600M$.

The second numerical experiment did not show stability as the head-on collision after the ringdown phase. Higher values for the initial momentum and spin also did not produce accurate simulations, once they set large curvature amplitude that destabilises the performance by the need for more numerical resolution. This problem may be bypassed implementing grid refinement methods to increase the accuracy of evolution equations. In the next chapter, we will discuss further improvements that may be made to our numerical code.

Chapter 6

General discussion

The 3+1 formalism has been in the last twenty years an exceptional mathematical tool that expanded the investigation of Cauchy problems and the study of gravitational dynamics in General Relativity (GR). With this mechanism, it was possible to develop a theory of canonical quantum gravity, thanks to the ADM formalism, which later gives rise to the Loop Quantum Gravity theory that is still in progress. Meanwhile, the same formalism was also used to study numerical solutions for GR, which made possible to simulate the spacetime in various regimes and established another new subarea in Gravitation, the Numerical Relativity.

In this dissertation, we presented an introduction to 3+1 formalism, studied initial data for some regimes and applied this knowledge in two numerical experiments to evolve the spacetime using the 3+1 Einstein equation. We choose a binary black hole as a system to simulate the metric in a head-on collision and a smooth ellipsoidal collision. In this set of equations there are no energy-momentum tensor components, and thus we did not evaluate any equation of motion – what reduced the computational cost.

Moreover, we implemented only second-order accuracy in the finite differencing operators, since higher orders showed no improvement. This circumstance is concerning to the value defined for the gridspacing; to improve the simulation resolution, we need to set a more refined value to it – without loose numerical stability. Although this procedure allows us to write fourth-order accuracy operators, the computational cost is overly large to the purpose of this dissertation. As an alternative solution for future works,

one can implement the Adaptive Mesh Refinement (AMR), in which the gridspacing is dynamically refined according to the spatial curvature magnitude since the closer gridpoints are from punctures, the finer is the gridspacing.

We took advantage of the system symmetry to perform two-dimensional simulations as a way to speed up the achievement of results. On another hand, it is not convenient to obtain physical measurements, as final total mass, total angular momentum and gravitational waves (GW)s once they depend on integrations of the hypersurface volume. Thereby, as future improvement in this numerical code one may implement the AMR to perform efficient three-dimensional grids. This update will allow us to measure the energy spent on GWs and study the conservation of linear and angular momentum of coalescing compact objects.

The numerical measurement of GWs, furthermore, enables us to expand the study of spacetime dynamics regarding the real measurement of GWs by interferometers. Numerical Relativity (NR) is part of our theoretical apparatus that will aid us expanding the investigation of astrophysical objects within the limits of GR. We may test Einstein theory by comparing GW data with, for instance, theories in which the speed of GW is different from the light or even theories that present other modes of GW polarisation.

Before the first detection of these spacetime ripples, the whole astrophysical measurements were got only from electromagnetic waves (EW)s, but now, GWs open a new sense to know the cosmos around us. From GW data we may establish a new standard candle to measure cosmological distance in which these gravitational sources also emit EW, as a way to make a precise measurement of the Hubble constant. This technique will make possible to obtain closer values to the abundance of dark matter and dark energy. In this study, NR will be necessary to simulate astrophysical conditions, performing the right-hand side of Einstein equation and hydrodynamic equations of motion. In addition, NR may help us to understand GW data from the early universe to obtain information beyond cosmic microwave background – nanosecond after the Big Bang – and discover a new cosmology or even a new physics.

Appendix A

Hamiltonian formulation of 3+1 GR

The original description of Einstein field equation in ADM formalism is an attempt to formulate the Hamiltonian to obtain a quantum description of gravity [11]. The authors Arnowitt, Deser and Misner split up the spacetime into hypersurfaces of constant time intervals and wrote the line element as following,

$$ds^2 = -(\alpha^2 - \beta_i\beta^i)\, c^2dt^2 + 2\beta_i\, cdt\, dx^i + \gamma_{ij}\, dx^i dx^j\,. \tag{A.1}$$

As discussed previously, the Lagrangian of the geometrical part of Einstein equation is $L = R$, in which the scalar curvature is a four-dimensional field [95]. To portray it in terms of its projection into a hypersurface Σ_t, we will contract the Gauss-Codazzi equation (3.18) twice to get that

$$\gamma^{\mu\sigma}\gamma^{\nu\rho}R_{\mu\nu\sigma\rho} = {}^{(3)}R + K^2 - K_{\mu\nu}K^{\mu\nu}\,; \quad (\gamma^{\mu\nu} = g^{\mu\nu} + n^\mu n^\nu) \tag{A.2}$$

$$R + 2\, n^\mu n^\nu R_{\mu\nu} = {}^{(3)}R + K^2 - K_{\mu\nu}K^{\mu\nu}\,; \quad (n^\mu n^\nu R_{\mu\nu} = 2n^\mu\nabla_{[\nu}\nabla_{\mu]}n^\nu) \tag{A.3}$$

$$\therefore\ R = {}^{(3)}R - K^2 + K_{\mu\nu}K^{\mu\nu} + 2\nabla_\mu\left(n^\nu\nabla_\nu n^\mu - n^\mu\nabla_\nu n^\nu\right)\,. \tag{A.4}$$

The equation above is what we are looking for; however, the last term on the right-hand side can be negligible. To understand why we can omit it, let us write the Einstein-

Hilbert action,

$$S = \int_{\mathcal{M}} [\,{}^{(3)}R - K^2 + K_{\mu\nu}K^{\mu\nu} + 2\nabla_\mu\left(n^\nu\nabla_\nu n^\mu - n^\mu\nabla_\nu n^\nu\right)]\sqrt{-g}\,d^4x\,. \tag{A.5}$$

Taking advantage of the *divergence theorem* in the variation of the action, we have that

$$\begin{aligned}
\delta S &= \delta(\cdots)_{\mathcal{M}} + 2\,\delta\int_{\mathcal{M}} \nabla_\mu\left(n^\nu\nabla_\nu n^\mu - n^\mu\nabla_\nu n^\nu\right)\sqrt{-g}\,d^4x\,, && \text{(A.6)}\\
&= \delta(\cdots)_{\Sigma} + 2\,\delta\int_{\Sigma} n_\mu\left(n^\nu\nabla_\nu n^\mu - n^\mu\nabla_\nu n^\nu\right)\gamma^{1/2}\,d^3x\,; \quad (n_\mu\nabla_\nu n^\mu = 0) && \text{(A.7)}\\
&= \delta(\cdots)_{\Sigma} + 2\,\delta\int_{\Sigma} \nabla_\nu n^\nu \gamma^{1/2}\,d^3x\,, \quad {}^{0} && \text{(A.8)}\\
&= \delta\int_{\mathcal{M}} \left({}^{(3)}R - K^2 + K_{\mu\nu}K^{\mu\nu}\right)\sqrt{-g}\,d^4x\,. && \text{(A.9)}
\end{aligned}$$

The term that was set as null is the extrinsic curvature, which vanishes at the boundary of the hypersurface – where spacetime is asymptotically flat. Thereby, we define the Lagrangian of the 3+1 GR written as

$$\boxed{L \doteqdot {}^{(3)}R - K^2 + K_{ij}K^{ij}}\,. \tag{A.10}$$

The *total* Hamiltonian H will be defined as the volume integral of the Hamiltonian *density* $\mathcal{H}$ [11],

$$H = \int_\Sigma \mathcal{H}\,d^3x\,, \tag{A.11}$$

$$\mathcal{H} \doteqdot \pi^{ij}\,\dot{\gamma}_{ij} - \mathcal{L}\,, \tag{A.12}$$

where $\mathcal{L} = \alpha\,\gamma^{1/2}L$ is the Lagrangian density and the *canonical momenta* π^{ij} is given by

$$\begin{aligned}
\pi^{ij} &\doteqdot \frac{\partial\mathcal{L}}{\partial\dot{\gamma}_{ij}}\,; \quad (\dot{\gamma}_{ij} = \pounds_{\vec{\beta}}\gamma_{ij} - 2\alpha K_{ij}) && \text{(A.13)}\\
&= -\gamma^{1/2}(K^{ij} - K\gamma^{ij})\,. && \text{(A.14)}
\end{aligned}$$

Its trace is $\pi \doteqdot \gamma_{ij}\pi^{ij} = 2\,\gamma^{1/2}K$, and the extrinsic curvature can be rewritten as

$$\boxed{K^{ij} = -\gamma^{-1/2}\left(\pi^{ij} - \tfrac{1}{2}\pi\gamma^{ij}\right)}\,. \tag{A.15}$$

Thereby, the Hamiltonian density is written

$$\mathcal{H} = 2\pi^{ij}D_{(i}\,\beta_{j)} - \alpha\,\gamma^{1/2}\left({}^{(3)}R + K^2 - K_{ij}K^{ij}\right)\,. \tag{A.16}$$

The evolution equations for this quantum descrition of Einstein field equation are written as following,

$$\begin{aligned}
\dot{\gamma}_{ij} &\doteqdot \frac{\delta H}{\delta \pi^{ij}}\,, && \text{(A.17)}\\
&= 2\alpha\gamma^{-1/2}\left(\pi_{ij} - \tfrac{1}{2}\pi\gamma_{ij}\right) + 2D_{(i}\beta_{j)}\,. && \text{(A.18)}
\end{aligned}$$

$$\begin{aligned}
\dot{\pi}^{ij} &\doteqdot -\frac{\delta H}{\delta \gamma_{ij}}\,, && \text{(A.19)}\\
&= -\alpha\gamma^{1/2}\left({}^{(3)}R^{ij} - \tfrac{1}{2}\,{}^{(3)}R\gamma^{ij}\right) + \tfrac{1}{2}\alpha\gamma^{-1/2}\gamma^{ij}\left(\pi_{ij}\pi^{ij} - \tfrac{1}{2}\pi^2\right)\\
&- 2\alpha\gamma^{-1/2}\left(\pi^{ik}\pi_k^{\ j} - \tfrac{1}{2}\pi\pi^{ij}\right) + \gamma^{1/2}\left(D^iD^j\alpha - \gamma^{ij}D^kD_k\alpha\right)\\
&+ D_k\left(\beta^k\pi^{ij}\right) - 2\pi^{k(i}D_k\beta^{j)}\,. && \text{(A.20)}
\end{aligned}$$

Equations (A.18) and (A.20) evolve a quantum regime in a sourceless region of the hypersurface Σ_t, which is analogous to the Schwarzschild spacetime.

Bibliography

[1] Edward Grant. The foundations of modern science in the middle ages. pages 1–60. Cambridge University Press, 1996.

[2] Olaf Pedersen. Early physics and astronomy. page 130. Cambridge University Press, 1993.

[3] Clifford Pickover. Archimedes to hawking: Laws of science and the great minds behind them. Oxford University Press, 2008.

[4] Mainak Kumar Bose. Late classical india. page 351. A. Mukherjee & Co, 1988.

[5] I. Bernard Cohen and George E. Smith, editors. *The Cambridge Companion to Newton*. Cambridge University Press, 2002. doi: 10.1017/ccol0521651778.

[6] Calvin J. Hamilton. Views of the solar system. 2007.

[7] title = Space Race: The Epic Battle Between America and the Soviet Union Deborah Cadbury. page 351. Paperback, 2007.

[8] Albert et al Einstein. *The collected papers of Albert Einstein*. Princeton University Press, 1 edition, 2009.

[9] Georges Darmois. Les équation de la gravitation einsteinienne. (25), 1927.

[10] Lichnerowicz III. L'intégration des équations de la gravitation relativiste et le probléme des n corps. *J. Math. pures el appl.*, pages 37–62, 1944.

[11] Richard Arnowitt, Stanley Deser, and Charles W. Misner. Republication of: The dynamics of general relativity. *General Relativity and Gravitation*, 40(9):1997–2027, aug 2008. doi: 10.1007/s10714-008-0661-1.

[12] Susan G Hahn and Richard W Lindquist. The two-body problem in geometrodynamics. *Annals of Physics*, 29(2):304–331, sep 1964. doi: 10.1016/0003-4916(64)90223-4.

[13] H. O'Hanian. *Einstein's Mistakes - The Human Failings of Genius*. W. W. Norton, 2008.

[14] Matthias Blau. Lecture notes on general relativity, 2016.

[15] Senta Troemel-Ploetz. Mileva einstein-marić. *Women's Studies International Forum*, 13(5):415–432, jan 1990. doi: 10.1016/0277-5395(90)90094-e.

[16] A. Einstein. Die feldgleichungen der gravitation. In *Albert Einstein: Akademie-Vorträge*, pages 88–92. Wiley-VCH Verlag GmbH & Co. KGaA, sep 2006. doi: 10.1002/3527608958.ch5.

[17] Origins of the expanding universe: 1912-1932, 2013.

[18] Edwin Hubble. Effects of red shifts on the distribution of nebulae. *The Astrophysical Journal*, 84:517, dec 1936. doi: 10.1086/143782.

[19] B. P. Abbott, R. Abbott, T. D. Abbott, M. R. Abernathy, F. Acernese, K. Ackley, C. Adams, and T. Adams. Observation of gravitational waves from a binary black hole merger. *Physical Review Letters*, 116(6), feb 2016. doi: 10.1103/physrevlett.116.061102.

[20] John C. Baez and Emory F. Bunn. The meaning of einstein's equation. *American Journal of Physics*, 73(7):644–652, jul 2005. doi: 10.1119/1.1852541.

[21] David B. Fairlie. Geometry, topology and physics. *Bulletin of the London Mathematical Society*, 23(3):319–320, may 1991. doi: 10.1112/blms/23.3.319.

[22] Lee C. Loveridge. Physical and geometric interpretations of the riemann tensor, ricci tensor, and scalar curvature. jan 2004. URL https://arxiv.org/abs/gr-qc/0401099.

[23] K. Schwarzschild. On the gravitational field of a mass point according to Einstein's theory. *ArXiv Physics e-prints*, May 1999.

[24] K. Schleich and D. M. Witt. What does Birkhoff's theorem really tell us? *ArXiv e-prints*, October 2009.

[25] S. Deser. Stressless schwarzschild. *General Relativity and Gravitation*, 46(1), dec 2013. doi: 10.1007/s10714-013-1615-9.

[26] Saul A Teukolsky. The kerr metric. *Classical and Quantum Gravity*, 32(12):124006, jun 2015. doi: 10.1088/0264-9381/32/12/124006.

[27] J. R. Oppenheimer and G. M. Volkoff. On massive neutron cores. *Physical Review*, 55(4):374–381, feb 1939. doi: 10.1103/physrev.55.374.

[28] A. Friedman. Uber die krummung des raumes. *Zeitschrift fur Physik*, 10(1): 377–386, dec 1922. doi: 10.1007/bf01332580.

[29] H. Poincaré. On the dynamics of the electron. July 1905.

[30] Kip S. Thorne Charles W. Misner John Archibald Wheeler. *Gravitation*, volume 1. W.H.Freeman & Co Ltd, 1973.

[31] Miguel Alcubierre. *Introduction to 3+1 Numerical Relativity*. International Series of Monographs on Physics. Oxford University Press, USA, oup edition, 2008.

[32] Masaru Shibata. *Numerical Relativity*. 100 Years of General Relativity. World Scientific Publishing Co, 2015.

[33] Stuart L. Shapiro Thomas W. Baumgarte. *Numerical relativity: solving Einstein's equations on the computer*. Cambridge University Press, 2010.

[34] Sean Carroll. *Spacetime and geometry: an introduction to General Relativity*. Benjamin Cummings, 2004.

[35] Sayan Kar and Soumitra Sengupta. The raychaudhuri equations: A brief review. *Pramana*, 69(1):49–76, jul 2007. doi: 10.1007/s12043-007-0110-9.

[36] Simonetta Frittelli. Note on the propagation of the constraints in standard 3+1 general relativity. *Physical Review D*, 55(10):5992–5996, may 1997. doi: 10.1103/physrevd.55.5992.

[37] John David Jackson. *Classical electrodynamics*. Wiley, 3rd ed edition, 1999.

[38] Vitor Cardoso, Leonardo Gualtieri, Carlos Herdeiro, and Ulrich Sperhake. Exploring new physics frontiers through numerical relativity. *Living Reviews in Relativity*, 18(1), sep 2015. doi: 10.1007/lrr-2015-1.

[39] S. L. Shapiro and S. A. Teukolsky. Black holes, star clusters, and naked singularities: Numerical solution of einstein's equations. *Philosophical Transactions of the Royal Society A: Mathematical, Physical and Engineering Sciences*, 340(1658):365–390, sep 1992. doi: 10.1098/rsta.1992.0073.

[40] M. Shibata. Fully general relativistic simulation of merging binary clusters: Spatial gauge condition. *Progress of Theoretical Physics*, 101(6):1199–1233, jun 1999. doi: 10.1143/ptp.101.1199.

[41] James R. Wilson. Numerical study of fluid flow in a kerr space. *The Astrophysical Journal*, 173:431, apr 1972. doi: 10.1086/151434.

[42] José A. Font, Mark Miller, Wai-Mo Suen, and Malcolm Tobias. Three-dimensional numerical general relativistic hydrodynamics: Formulations, methods, and code tests. *Physical Review D*, 61(4), jan 2000. doi: 10.1103/physrevd.61.044011.

[43] Zhoujian Cao, Hwei-Jang Yo, and Jui-Ping Yu. Reinvestigation of moving punctured black holes with a new code. *Physical Review D*, 78(12), dec 2008. doi: 10.1103/physrevd.78.124011.

[44] Alessandra Buonanno, Gregory B. Cook, and Frans Pretorius. Inspiral, merger, and ring-down of equal-mass black-hole binaries. *Physical Review D*, 75(12), jun 2007. doi: 10.1103/physrevd.75.124018.

[45] Masaru Shibata. Fully general relativistic simulation of coalescing binary neutron stars: Preparatory tests. *Physical Review D*, 60(10), oct 1999. doi: 10.1103/physrevd.60.104052.

[46] Luca Baiotti, Bruno Giacomazzo, and Luciano Rezzolla. Accurate evolutions of inspiralling neutron-star binaries: Prompt and delayed collapse to a black hole. *Physical Review D*, 78(8), oct 2008. doi: 10.1103/physrevd.78.084033.

[47] Zachariah B. Etienne, Yuk Tung Liu, Stuart L. Shapiro, and Thomas W. Baumgarte. General relativistic simulations of black-hole–neutron-star mergers: Effects of black-hole spin. *Physical Review D*, 79(4), feb 2009. doi: 10.1103/physrevd.79.044024.

[48] Nigel T. Bishop and Luciano Rezzolla. Extraction of gravitational waves in numerical relativity. *Living Reviews in Relativity*, 19(1), oct 2016. doi: 10.1007/s41114-016-0001-9.

[49] John G. Baker, Joan Centrella, Dae-Il Choi, Michael Koppitz, and James van Meter. Gravitational-wave extraction from an inspiraling configuration of merging black holes. *Physical Review Letters*, 96(11), mar 2006. doi: 10.1103/physrevlett.96.111102.

[50] Tristan L. Smith, Elena Pierpaoli, and Marc Kamionkowski. New cosmic microwave background constraint to primordial gravitational waves. *Physical Review Letters*, 97(2), jul 2006. doi: 10.1103/physrevlett.97.021301.

[51] Christophe Ringeval and Teruaki Suyama. Stochastic gravitational waves from cosmic string loops in scaling. *Journal of Cosmology and Astroparticle Physics*, 2017(12):027–027, dec 2017. doi: 10.1088/1475-7516/2017/12/027.

[52] Zhoujian Cao, Pablo Galaviz, and Li-Fang Li. Binary black hole mergers inf(r)theory. *Physical Review D*, 87(10), may 2013. doi: 10.1103/physrevd.87.104029.

[53] Mark A. Scheel, Stuart L. Shapiro, and Saul A. Teukolsky. Collapse to black holes in brans-dicke theory. II. comparison with general relativity. *Physical Review D*, 51(8):4236–4249, apr 1995. doi: 10.1103/physrevd.51.4236.

[54] A.E. Bernardini and O. Bertolami. The hamiltonian formalism for scalar fields coupled to gravity in a cosmological background. *Annals of Physics*, 338:1–20, nov 2013. doi: 10.1016/j.aop.2013.07.003.

[55] S W Hawking and Gary T Horowitz. The gravitational hamiltonian, action, entropy and surface terms. *Classical and Quantum Gravity*, 13(6):1487–1498, jun 1996. doi: 10.1088/0264-9381/13/6/017.

[56] M.A. Vasiliev. Consistent equations for interacting gauge fields of all spins in 3+1 dimensions. *Physics Letters B*, 243(4):378–382, jul 1990. doi: 10.1016/0370-2693(90)91400-6.

[57] James W. York. Gravitational degrees of freedom and the initial-value problem. *Physical Review Letters*, 26(26):1656–1658, jun 1971. doi: 10.1103/physrevlett.26.1656.

[58] James W. York. Role of conformal three-geometry in the dynamics of gravitation. *Physical Review Letters*, 28(16):1082–1085, apr 1972. doi: 10.1103/physrevlett.28.1082.

[59] Eric Gourgoulhon. *3+1 Formalism in General Relativity - Bases of Numerical Relativity*. Springer, 2012.

[60] A. N. Lasenby M. P. Hobson, G. P. Efstathiou. *General relativity: an introduction for physicists*. Cambridge University Press, 2005.

[61] James W. York. Conformal thin-sandwich data for the initial-value problem of general relativity. *Physical Review Letters*, 82(7):1350–1353, feb 1999. doi: 10.1103/physrevlett.82.1350.

[62] Thomas W. Baumgarte, Niall Ó Murchadha, and Harald P. Pfeiffer. Einstein constraints: Uniqueness and nonuniqueness in the conformal thin sandwich approach. *Physical Review D*, 75(4), feb 2007. doi: 10.1103/physrevd.75.044009.

[63] Larry Smarr and James W. York. Kinematical conditions in the construction of spacetime. *Physical Review D*, 17(10):2529–2551, may 1978. doi: 10.1103/physrevd.17.2529.

[64] Jeffrey M. Bowen and James W. York. Time-asymmetric initial data for black holes and black-hole collisions. *Physical Review D*, 21(8):2047–2056, apr 1980. doi: 10.1103/physrevd.21.2047.

[65] Reinaldo J. Gleiser, Carlos O. Nicasio, Richard H. Price, and Jorge Pullin. Evolving the bowen-york initial data for spinning black holes. *Physical Review D*, 57(6):3401–3407, mar 1998. doi: 10.1103/physrevd.57.3401.

[66] Ken ichi Oohara, Takashi Nakamura, and Masaru Shibata. Chapter 3. a way to 3d numerical relativity. *Progress of Theoretical Physics Supplement*, 128:183–249, 1997. doi: 10.1143/ptps.128.183.

[67] Larry Smarr and James W. York. Radiation gauge in general relativity. *Physical Review D*, 17(8):1945–1956, apr 1978. doi: 10.1103/physrevd.17.1945.

[68] Frans Pretorius. Numerical relativity using a generalized harmonic decomposition. *Classical and Quantum Gravity*, 22(2):425–451, jan 2005. doi: 10.1088/0264-9381/22/2/014.

[69] Frans Pretorius. Evolution of binary black-hole spacetimes. *Physical Review Letters*, 95(12), sep 2005. doi: 10.1103/physrevlett.95.121101.

[70] Miguel Alcubierre and Joan Masso. Pathologies of hyperbolic gauges in general relativity and other field theories. *Phys.Rev.D Rapid Comm*, (5), set 1997. doi: 10.1103/PhysRevD.57.4511.

[71] A M Khokhlov and I D Novikov. Gauge stability of 3+1 formulations of general relativity. *Classical and Quantum Gravity*, 19(4):827–846, feb 2002. doi: 10.1088/0264-9381/19/4/314.

[72] Frans Pretorius. Numerical relativity using a generalized harmonic decomposition. *Classical and Quantum Gravity*, 22(2):425–451, jan 2005. doi: 10.1088/0264-9381/22/2/014.

[73] Carles Bona, Joan Massó, Edward Seidel, and Joan Stela. New formalism for numerical relativity. *Physical Review Letters*, 75(4):600–603, jul 1995. doi: 10.1103/physrevlett.75.600.

[74] Peter Anninos, Joan Massó, Edward Seidel, Wai-Mo Suen, and John Towns. Three-dimensional numerical relativity: The evolution of black holes. *Physical Review D*, 52(4):2059–2082, aug 1995. doi: 10.1103/physrevd.52.2059.

[75] Larry Smarr and James W. York. Radiation gauge in general relativity. *Physical Review D*, 17(8):1945–1956, apr 1978. doi: 10.1103/physrevd.17.1945.

[76] Miguel Alcubierre and Bernd Brügmann. Simple excision of a black hole in 3+1 numerical relativity. *Physical Review D*, 63(10), apr 2001. doi: 10.1103/physrevd.63.104006.

[77] Miguel Alcubierre, Bernd Brügmann, Denis Pollney, Edward Seidel, and Ryoji Takahashi. Black hole excision for dynamic black holes. *Physical Review D*, 64(6), aug 2001. doi: 10.1103/physrevd.64.061501.

[78] Miguel Alcubierre, Bernd Brügmann, Peter Diener, Michael Koppitz, Denis Pollney, Edward Seidel, and Ryoji Takahashi. Gauge conditions for long-term numerical black hole evolutions without excision. *Physical Review D*, 67(8), apr 2003. doi: 10.1103/physrevd.67.084023.

[79] James R. van Meter, John G. Baker, Michael Koppitz, and Dae-Il Choi. How to move a black hole without excision: Gauge conditions for the numerical evolution of a moving puncture. *Physical Review D*, 73(12), jun 2006. doi: 10.1103/physrevd.73.124011.

[80] Bernd Brügmann, José A. González, Mark Hannam, Sascha Husa, Ulrich Sperhake, and Wolfgang Tichy. Calibration of moving puncture simulations. *Physical Review D*, 77(2), jan 2008. doi: 10.1103/physrevd.77.024027.

[81] Dieter R. Brill and Richard W. Lindquist. Interaction energy in geometrostatics. *Physical Review*, 131(1):471–476, jul 1963. doi: 10.1103/physrev.131.471.

[82] Richard W. Lindquist. Initial-value problem on einstein-rosen manifolds. *Journal of Mathematical Physics*, 4(7):938–950, jul 1963. doi: 10.1063/1.1704020.

[83] Steven Brandt and Bernd Brügmann. A simple construction of initial data for multiple black holes. *Physical Review Letters*, 78(19):3606–3609, may 1997. doi: 10.1103/physrevlett.78.3606.

[84] Edward Seidel and Wai-Mo Suen. Towards a singularity-proof scheme in numerical relativity. *Physical Review Letters*, 69(13):1845–1848, sep 1992. doi: 10.1103/physrevlett.69.1845.

[85] Peter Anninos, Greg Daues, Joan Massó, Edward Seidel, and Wai-Mo Suen. Horizon boundary condition for black hole spacetimes. *Physical Review D*, 51(10):5562–5578, may 1995. doi: 10.1103/physrevd.51.5562.

[86] Masaru Shibata and Takashi Nakamura. Evolution of three-dimensional gravitational waves: Harmonic slicing case. *Physical Review D*, 52(10):5428–5444, nov 1995. doi: 10.1103/physrevd.52.5428.

[87] Thomas W. Baumgarte and Stuart L. Shapiro. Numerical integration of einstein's field equations. *Physical Review D*, 59(2), dec 1998. doi: 10.1103/physrevd.59.024007.

[88] Takashi Nakamura, Kenichi Oohara, and Yasufumi Kojima. General relativistic collapse to black holes and gravitational waves from black holes. *Progress of Theoretical Physics Supplement*, 90:1–218, 1987. doi: 10.1143/ptps.90.1.

[89] Vetterling W.T. Flannery B.P. Press W.H., Teukolsky S.A. *Numerical recipes in C: the art of scientific computing.* Cambridge University Press, 2nd ed edition, 1997.

[90] Saul A. Teukolsky. Stability of the iterated crank-nicholson method in numerical relativity. *Physical Review D*, 61(8), mar 2000. doi: 10.1103/physrevd.61.087501.

[91] Miguel Alcubierre, Bernd Brügmann, Thomas Dramlitsch, José A. Font, Philippos Papadopoulos, Edward Seidel, Nikolaos Stergioulas, and Ryoji Takahashi. Towards a stable numerical evolution of strongly gravitating systems in general relativity: The conformal treatments. *Physical Review D*, 62(4), jul 2000. doi: 10.1103/physrevd.62.044034.

[92] H. Kreiss and Joseph Oliger. Methods for the approximate solution of time dependent problems. page 107, 1973.

[93] M. Campanelli, C. O. Lousto, P. Marronetti, and Y. Zlochower. Accurate evolutions of orbiting black-hole binaries without excision. *Physical Review Letters*, 96(11), mar 2006. doi: 10.1103/physrevlett.96.111101.

[94] Thomas W. Baumgarte. Innermost stable circular orbit of binary black holes. *Physical Review D*, 62(2), jun 2000. doi: 10.1103/physrevd.62.024018.

[95] Robert M. Wald. *General relativity.* University of Chicago Press, first edition edition, 1984.